 doi:10.20944/preprints202010.0386.v1

Article

A computational model to inform effective control interventions against *Yersinia enterocolitica* coinfection

Reihaneh Mostolizadeh [1,2,3,4,*] and Andreas Dräger [1,2,3,4]

1 Computational Systems Biology of Infection and Antimicrobial-Resistant Pathogens, Institute for Bioinformatics and Medical Informatics (IBMI), University of Tübingen, 72076 Tübingen, Germany
2 Department of Computer Science, University of Tübingen, 72076 Tübingen, Germany
3 German Center for Infection Research (DZIF), partner site Tübingen, Germany
4 Cluster of Excellence 'Controlling Microbes to Fight Infections,' University of Tübingen
5 Institute for Clinical Epidemiology and Applied Biometry, University of Tübingen
6 Epimos GmbH
* Correspondence: mostoli@informatik.uni-tuebingen.de; phone: +49 7071 29-70488

Abstract: The complex interplay among pathogens, host factors, and the integrity and composition of the endogenous microbiome determine the course and outcome of gastrointestinal infections. The model organism *Yersinia entercolitica* (Ye) is one of the five top frequent causes of bacterial gastroenteritis based on the Epidemiological Bulletin of the Robert Koch Institute (RKI) published on September 10, 2020. A fundamental challenge in predicting the course of an infection is to understand whether co-infection with two *Yersinia* strains differing only in their capacity to resist killing by the host immune system may decrease the overall virulence by competitive exclusion or increase it by acting cooperatively. Herein, we study the primary interactions among Ye, the host immune system and the microbiota, and their influence on *Yersinia* population dynamics. The employed model considers two host compartments, the intestinal mucosa and lumen, commensal bacteria, the co-existence of wild-type and mutant *Yersinia* strains, as well the host immune responses. We determine four possible equilibria: the disease-free, wild-type-free, mutant-free, and co-existence of wild-type and mutant equilibrium. We also calculate the reproduction number for each strain as a threshold parameter to determine if the population may either be eradicated or persist within the host. We conclude that the infection should disappear if the reproduction numbers for each strain fall below one, and the commensal bacteria's growth rate exceeds the pathogens' growth rates. These findings will help inform medical control strategies. The supplement includes MATLAB source script, Maple workbook, and figures.

Keywords: Reproduction number; Disease-free equilibrium; Co-existence equilibrium; *Yersinia*; gastroenteritis

1. Introduction

Forecasting the evolution of infectious diseases is the primary motivation behind the use of mathematical models in biology. Determining those threshold values that predict whether the disease will spread within the host or can be contained is crucial to inform medical control strategies.

Yersinia entercolitica (Ye) is a Gram-negative enteropathogen causing foodborne gastrointestinal infections. Within the small intestine (SI), Ye can adhere to and invade the intestinal epithelial lining mainly via the adhesins Yersinia adhesin A (YadA) [1] and Invasin [2–4]. YadA is among the essential

 doi:10.20944/preprints202010.0386.v1

virulence factors as a YadA-deficient strain is impaired in 97 colonization and systemic spread in a mouse model of infection [5].

Upon attachment, Ye can engage its Type III secretion system (T3SS) to inject effector proteins, the *Yersinia* outer proteins (Yops), into host cells, thus evading the host immune response and establishing a productive infection [6,7]. Indeed, the first line of host defense against invading Ye is a massive infiltration of phagocytotic cells. However, Ye can counteract phagocytic killing via its T3SS [6,7].

Together, both the T3SS and YadA contribute to the efficient colonization of the intestinal tract, where Ye induces an inflammatory response that likely accounts for a reduction of density and complexity of the commensal microbiome [8,9].

Several Ye serotypes have been isolated from animal reservoirs and the human gastrointestinal tract, but only a few of them cause disease in humans. Although causing severe distress, gastrointestinal infections are generally self-contained. Typically, healthy persons will only receive symptomatic treatment aimed at avoiding dehydration. However, in individuals with underlying disease, elderly persons, or newborn children, gastrointestinal infections can cause high morbidity and even fatal outcomes. Especially in such patients, identifying those individuals who are at high risk of developing fatal diseases could help tailor personalized therapeutic interventions to improve the outcome of infection. To this aim, we recently developed a computational model that can calculate Ye population dynamics during gastrointestinal infection, predict pathogen expansion, gut colonization, and infection course [10].

Previously published models have focused on the evolution of virulence during co-infection and superinfection by more than one pathogen [11–17]. Furthermore, Nurtay *et al.* investigated theoretical conditions in co-existence strains while their research focused on viral populations of wild-type and mutant [18].

Herein, we apply our computational model to predict the behavior of Ye population dynamics during the co-infection of mice by different Ye mutant (mut) strains lacking distinct virulence factors and a Ye wild-type strain in bacterial gastroenteritis. We perform the bifurcation analysis to show how the dynamics of the system change as multiple parameters are varied [19,20].

The existence of a backward bifurcation, i.e., the co-existence of a stable disease-free equilibrium with one or more stable endemic equilibria, has significant consequences on the process of producing medical policies aimed at eradicating or controlling an infectious disease within host [21]. A fundamental parameter in models displaying a backward bifurcation is the basic reproduction number R_0. R_0 represents the expected number of new infections caused within host or between-hosts at the start of entering a pathogen into the host. If $R_0 > 1$, after an initial introduction, the infection spreads within host/or between-hosts, thus creating an infectious disease. If $R_0 < 1$, small initial introductions are not sufficiently transmissible to spread the infection within the host (or between hosts), and the cells get infected within a host. This is literally called an endemic disease that will fade out. Thus, many control policies like medication/vaccination have focused on reaching coverage levels sufficient to reduce R_0 below 1 [15,16,22,23]. Therefore, in this analysis, we compute the system's equilibrium points, study their stability and the center manifold, and investigate how the different points would affect the infection rate, virulence, and mutation rate. Next, we calculate the basic reproductive number for scenarios in which multiple strains are introduced, and an R_0 number is calculated for each strain. Finally, we discuss the biological implications of our results.

2. Materials and Methods

2.1. Model description

Our model for Ye, as described in Geißert *et al.* [10], considers three different sites with their individual population dynamics. The lumen and the mucosal site of the small intestine are illustrated as two separate compartments by abbreviated notations L and M in table 1. The mucosa and lumen

Preprints (www.preprints.org) | NOT PEER-REVIEWED | Posted: 19 October 2020 doi:10.20944/preprints202010.0386.v1

sites include three different population dynamics: commensal bacteria, wild-type *Yersinia*, and mutant *Yersinia*.

Table 1. The variable symbols and their meaning. The lumen is abbreviated with L, the mucosa as M. We also indicate each variable with mut or wild-type (wt) to denote to which population they refer. An upper-case I refers to the immune system.

Variable Symbol	Meaning	Units
B_M	Commensal bacteria in the mucosa	item
$Y_M^{(wt)}$	Wild-type *Yersinia* in the mucosa	item
$Y_M^{(mut)}$	Mutant *Yersinia* in the mucosa	item
B_L	Commensal bacteria in the lumen	item
$Y_L^{(wt)}$	Wild-type *Yersinia* in the lumen	item
$Y_L^{(mut)}$	Mutant *Yersinia* in the lumen	item
I	Strength of immune reaction	dimensionless

Besides the bacterial populations, we have the strength of the host immune response on the other side. For the sake of clarity, the complex immune cell population dynamics which is made up of innate and adaptive immunity are implemented in our model as a single abstract immune response in table 1. An advantage of this rather abstract immune response is that it is easily adjustable. Only the Ye populations in the mucosa activate the immune response, whereas tolerance to commensal bacteria exists. However, this immune response affects all bacterial populations at the mucosal site.

Upon oral co-infection, a Ye population enters the small intestinal lumen. Due to their particular virulence traits, some Ye cells are also able to enter the mucosal site.

As shown in the model eqs. (1) to (7), the population dynamics of bacterial species consist of both growth, i.e., an increase of populations due to a distinct growth rate α, and a reduction through peristalsis, which moves the bacterial populations towards the colon where they finally end up in feces. Peristalsis will only influence the populations in the lumen. Furthermore, bacterial populations in the mucosa can additionally be reduced through killing by the host immune attack.

Both sites, the lumen and the mucosal site, are colonized by commensal bacterial species but to a different extent. The colonization capacity of the lumen considerably exceeds that of the mucosal site. This is due to the host's natural mechanisms to limit bacterial contact to the epithelium through physical barriers, like the adherent mucus layer and a high concentration of anti-microbial peptides (AMPs). Hence, we assume a much lower carrying capacity of the mucosal site compared to the luminal compartment. Another assumption is that as soon as bacterial numbers exceed the mucosa's carrying capacity, they spill-over to the luminal site, feeding the luminal populations [10].

The model's immune system represented by I (see table 1) is activated as soon as at least one Ye cell enters the small intestinal mucosal compartment. This immune activation increases with the number of Ye cells in the mucosa. By triggering the killing of all bacterial cells at the mucosal site, this leads to a reduction of bacterial populations spilling over to the lumen [10].

In contrast to commensal bacteria, Ye exhibits a number of virulence traits to evade the host immune response. This is implemented in our model by different immunity adjustment factors for either the wild-type strain or the different mutant strains. Consequently, the number of commensal species is more affected by the host immune attack than the number of Ye mutant strains, which are, of course, more affected than the wild-type strain. Our model's final output is the number of bacteria or colony-forming units (CFUs), finally ending up in feces. These population dynamics are represented as the following a system of differential equations [10]:

$$\frac{\mathrm{d}}{\mathrm{d}t} B_M = \left(\alpha^{(B)} - \sigma^{(B)}_{M\longrightarrow L} - \gamma \cdot I\right) \cdot B_M \tag{1}$$

$$\frac{\mathrm{d}}{\mathrm{d}t} Y_M^{(wt)} = \left(\alpha^{(wt)} - \sigma^{(wt)}_{M\longrightarrow L} - \gamma \cdot f_I^{(wt)} \cdot I\right) \cdot Y_M^{(wt)} \tag{2}$$

Preprints (www.preprints.org) | NOT PEER-REVIEWED | Posted: 19 October 2020 doi:10.20944/preprints202010.0386.v1

$$\frac{\mathrm{d}}{\mathrm{d}t}Y_M^{(mut)} = \left(\alpha^{(mut)} - \sigma_{M\longrightarrow L}^{(mut)} - \gamma \cdot f_I^{(mut)} \cdot I\right) \cdot Y_M^{(mut)} \tag{3}$$

$$\frac{\mathrm{d}}{\mathrm{d}t}B_L = \left(\alpha_L^{(B)} - \beta\right) \cdot B_L + \sigma_{M\longrightarrow L}^{(B)} \cdot B_M \tag{4}$$

$$\frac{\mathrm{d}}{\mathrm{d}t}Y_L^{(wt)} = \left(\alpha_L^{(wt)} - \beta\right) \cdot Y_L^{(wt)} + \sigma_{M\longrightarrow L}^{(wt)} \cdot Y_M^{(wt)} \tag{5}$$

$$\frac{\mathrm{d}}{\mathrm{d}t}Y_L^{(mut)} = \left(\alpha_L^{(mut)} - \beta\right) \cdot Y_L^{(mut)} + \sigma_{M\longrightarrow L}^{(mut)} \cdot Y_M^{(mut)} \tag{6}$$

$$\frac{\mathrm{d}}{\mathrm{d}t}I = \left(Y_M^{(wt)} + Y_M^{(mut)}\right) \cdot \kappa \cdot \frac{C_I - I}{C_I}. \tag{7}$$

For a detailed description of the parameters, see table 2. Besides the seven differential equations describing the population dynamics of the Ye strains, the commensal bacteria and the immune system at the mucosal site, and all three populations (commensal bacteria, wild-type *Yersinia*, and mutant *Yersinia*) at the luminal site, the model consists of different mass-action terms describing the spill-over rates from the mucosa into the lumen and describing the growth rates of the bacterial populations, which are limited through a given capacity "C" and are defined as follows:

$$\sigma_{M\longrightarrow L}^{(B)} = \alpha^{(B)} \frac{B_M + Y_M^{(wt)} + Y_M^{(mut)}}{C_M} \quad \text{Spill-over rate commensal} \tag{8}$$

$$\sigma_{M\longrightarrow L}^{(wt)} = \alpha^{(wt)} \frac{B_M + Y_M^{(wt)} + Y_M^{(mut)}}{C_M} \quad \text{Spill-over rate wild-type} \tag{9}$$

$$\sigma_{M\longrightarrow L}^{(mut)} = \alpha^{(mut)} \frac{B_M + Y_M^{(wt)} + Y_M^{(mut)}}{C_M} \quad \text{Spill-over rate mutant} \tag{10}$$

$$\alpha_L^{(B)} = \alpha^{(B)} \frac{C_L - \left(B_L + Y_L^{(wt)} + Y_L^{(mut)}\right)}{C_L} \quad \text{Bacteria growth rate in the lumen} \tag{11}$$

$$\alpha_L^{(wt)} = \alpha^{(wt)} \frac{C_L - \left(B_L + Y_L^{(wt)} + Y_L^{(mut)}\right)}{C_L} \quad \text{Wild-type growth rate in the lumen} \tag{12}$$

$$\alpha_L^{(mut)} = \alpha^{(mut)} \frac{C_L - \left(B_L + Y_L^{(wt)} + Y_L^{(mut)}\right)}{C_L} \quad \text{Mutant growth rate in the lumen} \tag{13}$$

and model parameters are shown in table 2. Since the system is the modeling of *Yersinia* population in

Table 2. Definition of the parameters

Parameter	Definition	Unit
$\alpha^{(B)}$	Maximal growth rate of intestinal bacteria	1/h
$\alpha^{(wt)}$	Maximal growth rate of wild-type *Yersinia*	1/h
$\alpha^{(mut)}$	Maximal growth rate of mutant *Yersinia*	1/h
$f_I^{(wt)}$	Immunity adjustment factor for wild-type *Yersinia*	dimensionless
$f_I^{(mut)}$	Immunity adjustment factor for mutant *Yersinia*	dimensionless
C_M	Carrying capacity of the mucosa	item
C_L	Carrying capacity of the lumen	item
C_I	Carrying capacity of the immune system	item
γ	Maximal immunity action	1/h
κ	Maximal rate of immune growth	1/h
β	Rate at which intestines are discharged	1/h

the mucosa and lumen, we assume that all state variables and parameters of the model are non-negative $\forall t \geq 0$.

Preprints (www.preprints.org) | NOT PEER-REVIEWED | Posted: 19 October 2020 doi:10.20944/preprints202010.0386.v1

2.2. The basic reproduction number $\mathcal{R}_0$

The basic reproduction ratio $\mathcal{R}_0$ is calculated by the fraction of the transmission rate for each strain (spill-over) and the average infectious period for each strain in compartments as defined by Diekmann *et al.* [24].

In addition, van den Driessche and Watmough [25] defined $\mathcal{R}_0$ as a general compartmental disease transmission model suited to heterogeneous populations that can be modeled by a system of ordinary differential equations. The authors, thus, divided system $\dot{X} = f(X)$ as two different main compartments with the first compartment $\mathcal{F}_i(x)$ defined as the rate of the appearance of new infections in compartment i, $\mathcal{V}_i^+$ as the rate of transfer of individuals into compartment i by all other means, and $\mathcal{V}_i^-$ as the rate of transfer of individuals out of the compartment i where can be written as $\dot{x}_i = f_i(x) = \mathcal{F}_i(x) - \mathcal{V}_i, \quad i = 1, \ldots, n$. Therefore, the disease transmission model consisting of non-negative initial conditions will be as follows:

$$\frac{\mathrm{d}}{\mathrm{d}t} x_i = \mathcal{F}_i(x, y) - \mathcal{V}_i(x, y) \qquad \forall i \in \{1, \ldots, n\} \tag{14}$$

$$\frac{\mathrm{d}}{\mathrm{d}t} y_j = \mathcal{G}_j(x, y) \qquad \forall j \in \{1, \ldots, m\}. \tag{15}$$

It is assumed that functions $\mathcal{F}_i(x)$ and $\mathcal{V}_i = \mathcal{V}_i^- + \mathcal{V}_i^-$ are continuously differentiable at least twice in each variable, and they satisfy the assumptions items A(1) to A(5) described below [25,26]:

A(1) $\mathcal{F}_i(0, y) = \mathcal{V}_i(0, y) = 0 : \forall y > 0$ (no new infections if no infected)
A(2) $\mathcal{F}_i(x, y) \geq 0 : \forall x_i \geq 0 \wedge y_i \geq 0$ (no new infections if no infected)
A(3) $\mathcal{V}_i(0, y) \leq 0 : \forall y_i \geq 0$ (if compartment empty, can only have inflow)
A(4) $\sum_i \mathcal{V}_i(x, y) \geq 0 : \forall x_i \geq 0 \wedge y_i \geq 0$ (sum is net outflow)
A(5) The system $\dot{y} = \mathcal{G}(0, y)$ has unique asymptotically stable equilibrium, y^*

Theorem 1. *Consider the disease transmission model given by $\dot{X} = f(X)$ with $f(X)$ satisfying conditions items A(1) to A(5). If X_0 is a disease-free equilibrium (DFE) of the model, then X_0 is locally asymptotically stable if $\mathcal{R}_0 < 1$, but unstable if $\mathcal{R}_0 > 1$, where $\mathcal{R}_0$ acts as a threshold parameter.*

Proof. See [25]. □

Several models found in the literature have been used to show that when $\mathcal{R}_0$ crosses the threshold, $\mathcal{R}_0 = 1$, it can act as a bifurcation parameter and transcritical bifurcation takes place. That is, local asymptotical stability is transferred from the disease-free state to the new (positive) equilibria. In ordinary differential equations, we will encounter bifurcations of equilibrium and periodic orbits, which are typical in the sense that they occur when a small smooth change is made to the threshold parameter values (the bifurcation parameters μ) of a system. It causes a sudden qualitative or topological change in the behavior of the system. Consider the continuous dynamical system described by the Ordinary Differential Equation (ODE)

$$\dot{X} = f(X, \mu) \qquad \text{with } f : \mathbb{R}^n \times \mathbb{R} \to \mathbb{R}^n. \tag{16}$$

A local bifurcation occurs at (X_0, μ_0) if an eigenvalue with zero real part is included in the Jacobian matrix of the system. If the eigenvalue is equal to zero, the bifurcation is a steady-state bifurcation. Therefore, we now recall the analysis of the center manifold near the critically $(X = X_0, \mathcal{R}_0 = 1)$, which allows clarifying the direction of the bifurcation near the bifurcation point using the Center Manifold Theorem 2. This theory describes the determination of the local stability at the non-hyperbolic equilibrium (linearization matrix has at least one eigenvalue with zero real part) and the existence of another equilibrium (bifurcated from the non-hyperbolic equilibrium).

Preprints (www.preprints.org) | NOT PEER-REVIEWED | Posted: 19 October 2020 doi:10.20944/preprints202010.0386.v1

2.3. Center Manifold

The center manifold theorem provides a means for systematically reducing the dimension of the state spaces which need to be considered when analyzing bifurcations of a given type.

Theorem 2 (Center Manifold Theorem for Flows)**.** *Let f be a C^r vector field on $\mathbb{R}^n$ vanishing at the origin $f(0) = 0$ and let $A = Df(0)$. Divide the spectrum of A into three parts, $\sigma_s, \sigma_c, \sigma_u$ with*

$$Re\lambda \begin{cases} < 0 & if \quad \lambda \in \sigma_s \\ = 0 & if \quad \lambda \in \sigma_c \\ > 0 & if \quad \lambda \in \sigma_u \end{cases}. \tag{17}$$

Let the (generalized) eigenspaces of σ_s, σ_c and σ_u be E^s, E^c and E^u, respectively. Then there exist C^r stable and unstable invariant manifolds W^u and W^s tangent to E^u and E^s at 0 and a C^{r-1} center manifold W^c tangent to E^c at 0. The manifolds W^u, W^s and W^c are all invariant for the flow of f. The stable and unstable manifolds are unique, but W^c need not be.

Proof. See [27,28]. □

To achieve this, consider the general system

$$\dot{x} = Jx + F(x), \quad x \in \mathbb{R}^n \tag{18}$$

where Jx is the linear part of the system. We must first find the differential equations on its center manifold and then reduce the system to its normal form. Without loss of generality, we assume that $x = 0$ is the fixed point of interest for the system.

Suppose J has n_c eigenvalues with zero real-part and n_s eigenvalues with negative and positive real-part and $n = n_c + n_s$. Using the eigenvectors of J to form a transformation matrix, the system can be rewritten in block matrix form as

$$\begin{cases} \dot{x}_c &= Ax_c + f(x_c, x_s) \\ \dot{x}_s &= Bx_s + g(x_c, x_s) \end{cases} \tag{19}$$

where $(x_c, x_s) \in \mathbb{R}^{n_c} \times \mathbb{R}^{n_s}$, $A \in \mathbb{R}^{n_c} \times \mathbb{R}^{n_c}$ and $B \in \mathbb{R}^{n_s} \times \mathbb{R}^{n_s}$. With the eigenvalues of zero real-part, the Center Manifold Theorem 2 guarantees that there exists a smooth manifold $W_c = \{(x_c, x_s) \mid x_s = q(x_c)\}$ the equilibrium point such that the local behavior in the center direction of the system is qualitatively the same as that on the manifold. By differentiating $x_s = q(x_c)$, we get $\dot{x}_s = Dq(x_c)\dot{x}_c$. Substituting eq. (19) into the previous identity and rearranging the equation, we get

$$Dq(x_c)\left[Ax_c + f\left(x_c, q(x_c)\right)\right] - Bq(x_c) - g\left(x_c, q(x_c)\right) = 0. \tag{20}$$

By solving for $q(x_c)$, we get a function describing the center manifold. In general, $q(x_c)$ cannot be solved explicitly. Instead, substituting a Taylor expansion $q(x_c) = ax_c^2 + \mathcal{O}\left(x_c^3\right)$ into eq. (20), we can find the coefficients for the expansion by balancing the lower order terms. Based on $q(x_c)$, we now have a system in the reduced form:

$$\dot{x}_c = Ax_c + f\left(x_c, q(x_c)\right). \tag{21}$$

The following proposition helps us understand the type of transcritical bifurcation is forward or backward:

Proposition 1. *Assume that conditions items A(1) to A(5) are satisfied. Furthermore, assume that the following hypotheses are satisfied by the system in eqs.* (14) *to* (15)*:*

Preprints (www.preprints.org) | NOT PEER-REVIEWED | Posted: 19 October 2020 doi:10.20944/preprints202010.0386.v1

H(1) In the balance equations for the infected compartments, non-linear terms are present only in the rate of the appearance of new infections;
H(2) Nonlinear terms are bilinear;
H(3) There is no linear transfer from infected to uninfected compartments.

Then the transcritical bifurcation of the system in eqs. (14) to (15) at $\mathcal{R}_0 = 1$ is forward, and if at least one of these features is not present in the model structure, then a backward bifurcation may occur [26].

3. Results

We used the model in eqs. (1) to (7) to understand how the dynamics change following variation of different parameters. We calculated the equilibria of eqs. (1) to (7), conduct a linear stability analysis, and identified the analytical conditions that lead to a transcritical bifurcation.

3.1. Existence of equilibria

For mathematical convenience, we divide the model in eqs. (1) to (7) such that the first four equations correspond to infected individuals. The distinction between infected and uninfected populations must be determined from the model's epidemiological interpretation and cannot be deduced from the structure of the equations alone. Thus, we have

$$\frac{\mathrm{d}}{\mathrm{d}t}Y_M^{(wt)} = \left(\alpha^{(wt)} - \sigma_{M\longrightarrow L}^{(wt)} - \gamma \cdot f_I^{(wt)} \cdot I\right) \cdot Y_M^{(wt)} \tag{22}$$

$$\frac{\mathrm{d}}{\mathrm{d}t}Y_M^{(mut)} = \left(\alpha^{(mut)} - \sigma_{M\longrightarrow L}^{(mut)} - \gamma \cdot f_I^{(mut)} \cdot I\right) \cdot Y_M^{(mut)} \tag{23}$$

$$\frac{\mathrm{d}}{\mathrm{d}t}Y_L^{(wt)} = \left(\alpha_L^{(wt)} - \beta\right) \cdot Y_L^{(wt)} + \sigma_{M\longrightarrow L}^{(wt)} \cdot Y_M^{(wt)} \tag{24}$$

$$\frac{\mathrm{d}}{\mathrm{d}t}Y_L^{(mut)} = \left(\alpha_L^{(mut)} - \beta\right) \cdot Y_L^{(mut)} + \sigma_{M\longrightarrow L}^{(mut)} \cdot Y_M^{(mut)} \tag{25}$$

$$\frac{\mathrm{d}}{\mathrm{d}t}B_M = \left(\alpha^{(B)} - \sigma_{M\longrightarrow L}^{(B)} - \gamma \cdot I\right) \cdot B_M \tag{26}$$

$$\frac{\mathrm{d}}{\mathrm{d}t}B_L = \left(\alpha_L^{(B)} - \beta\right) \cdot B_L + \sigma_{M\longrightarrow L}^{(B)} \cdot B_M \tag{27}$$

$$\frac{\mathrm{d}}{\mathrm{d}t}I = \left(Y_M^{(wt)} + Y_M^{(mut)}\right) \cdot \kappa \cdot \frac{C_I - I}{C_I}, \tag{28}$$

while we assume that the growth rate $\alpha^{(B)}$ of the endogenous commensal bacteria is higher than the Ye growth rates $\alpha^{(wt)}$ and $\alpha^{(mut)}$, respectively.

On the other side, the *Yersinia* model has three compartments (mucosa, lumen, immune system), which are analyzed separately. The model system is analyzed in a suitable, feasible region. All forward solutions of the system are feasible $\forall t \geq 0$ if they enter the invariant region $\Omega = \Omega_L \times \Omega_M \times \Omega_I$ where

$$\Omega_L = \left(B_L, Y_L^{(wt)}, Y_L^{(mut)}\right) \in \mathbb{R}_+^3 : B_L + Y_L^{(wt)} + Y_L^{(mut)} \leq C_L \tag{29}$$

$$\Omega_M = \left(B_M, Y_M^{(wt)}, Y_M^{(mut)}\right) \in \mathbb{R}_+^3 : B_M + Y_M^{(wt)} + Y_M^{(mut)} \leq C_M \tag{30}$$

$$\Omega_I = (I) \in \mathbb{R}_+^1 : I \leq C_I. \tag{31}$$

The existence of equilibrium points for system eqs. (1) to (7) would be as follow:

- The trivial equilibrium point is as an origin equilibrium $(0, 0, 0, 0, 0, 0, 0)$. This solution appears when all populations are extinct. For all parameters, this point never becomes stable due to positivity of eigenvalues in A2.

Preprints (www.preprints.org) | NOT PEER-REVIEWED | Posted: 19 October 2020 doi:10.20944/preprints202010.0386.v1

- The first equilibrium point appears in the absence of *Yersinia* $Y_M^{(wt)} = Y_M^{(mut)} = Y_L^{(wt)} = Y_L^{(mut)} = 0$. System eqs. (1) to (7) has a disease-free equilibrium, which is given by

$$P^0 = \left(B_M^0, Y_M^{0(wt)}, Y_M^{0(mut)}, B_L^0, Y_L^{0(wt)}, Y_L^{0(mut)}, I^0\right) = \left(B_M^0, 0, 0, B_L^0, 0, 0, I^0\right) \tag{32}$$

and

$$B_M^0 = C_M\left(1 - \frac{\gamma}{\alpha^{(B)}}\right) \tag{33}$$

$$B_L^0 = C_L\left(1 - \frac{\beta}{\alpha^{(B)}}\right) \tag{34}$$

$$I^0 = 1. \tag{35}$$

It describes a disease-free state whereby only the commensal bacteria persist. In order for the disease-free state P^0 to be biologically meaningful, the conditions $\gamma < \alpha^{(B)}$ and $\beta < \alpha^{(B)}$ must hold. These conditions correspond to the maximal growth rate of intestinal bacteria exceeding the rate at which intestines are charged and the maximal immunity action, which is not that strong in the absence of *Yersinia* strains. However, the population of the immune system is in a maximum of its carrying capacity (in health, not in fighting with any infection).

- A second equilibrium corresponds to the commensal bacteria's persistence and the *Yersinia* mutant strain in the absence of the wild-type strain. Without loss of generality, the commensal bacteria are supposed to be zero because they are not infective. This point is obtained by setting $Y_M^{(wt)} = Y_L^{(wt)} = 0$:

$$P^{(mut)} = P^1 = \left(B_M^1, Y_M^{1(wt)}, Y_M^{1(mut)}, B_L^1, Y_L^{1(wt)}, Y_L^{1(mut)}, I^1\right) = \left(0, 0, Y_M^{1(mut)}, 0, 0, Y_L^{1(mut)}, C_I\right) \tag{36}$$

which

$$Y_M^{1(mut)} = C_M\left(1 - \frac{C_I\gamma f_I^{(mut)}}{\alpha^{(mut)}}\right) \tag{37}$$

$$Y_L^{1(mut)} = \frac{1}{2}\left(C_L\left(1 - \frac{\beta}{\alpha^{(mut)}}\right) + \sqrt{4C_MC_L\left(\frac{C_I\gamma f_I^{(mut)}}{\alpha^{(mut)}} - 1\right)^2 + C_L^2\left(1 - \frac{\beta}{\alpha^{(mut)}}\right)^2}\right). \tag{38}$$

- The other equilibrium corresponds to the persistence of commensal bacteria and the *Yersinia* wild-type strain in the absence of the mutant strain. Without loss of generality, the commensal bacteria are supposed to be zero because they are not infective. This point is obtained by setting $Y_M^{(mut)} = Y_L^{(mut)} = 0$:

$$P^{(wt)} = P^2 = \left(B_M^2, Y_M^{2(wt)}, Y_M^{2(mut)}, B_L^2, Y_L^{2(wt)}, Y_L^{2(mut)}, I^2\right) = \left(0, Y_M^{2(wt)}, 0, 0, Y_L^{2(wt)}, 0, C_I\right) \tag{39}$$

which

$$Y_M^{2(wt)} = C_M\left(1 - \frac{C_I\gamma f_I^{(wt)}}{\alpha^{(wt)}}\right) \tag{40}$$

$$Y_L^{2(wt)} = \frac{1}{2}\left(C_L\left(1 - \frac{\beta}{\alpha^{(wt)}}\right) + \sqrt{4C_MC_L\left(\frac{C_I\gamma f_I^{(wt)}}{\alpha^{(wt)}} - 1\right)^2 + C_L^2\left(1 - \frac{\beta}{\alpha^{(wt)}}\right)^2}\right). \tag{41}$$

Preprints (www.preprints.org) | NOT PEER-REVIEWED | Posted: 19 October 2020 doi:10.20944/preprints202010.0386.v1

- Finally, the last equilibrium point corresponds to a state of the co-existence of wild-type and mutant *Yersinia* strains. This point is achieved by supposing $B_M = B_L = 0$:

$$P^{(wt)(mut)} = P^3 = \left(B_M^3, Y_M^{3(wt)}, Y_M^{3(mut)}, B_L^3, Y_L^{3(wt)}, Y_L^{3(mut)}, I^3\right) = \left(0, Y_M^{3(wt)}, Z, 0, Y_L^{3(wt)}, Y_L^{3(mut)}, C_I\right) \quad (42)$$

with

$$Y_M^{3(wt)} = C_M\left(1 - \frac{C_I\gamma f_I^{(wt)}}{\alpha^{(wt)}}\right) - Z \quad (43)$$

$$Y_L^{3(wt)} = \frac{\alpha^{(mut)}\left(Z\left(1 - \frac{C_I\gamma f_I^{(wt)}}{\alpha^{(wt)}}\right) - \gamma f_I^{(wt)}\left(1 - \frac{C_I}{\alpha^{(wt)}}\right)^2\right)}{\beta\left(1 - \frac{\alpha^{(mut)}}{\alpha^{(wt)}}\right)} \quad (44)$$

$$Y_L^{3(mut)} = \frac{\alpha^{(mut)}\left(1 - \frac{C_I\gamma f_I^{(wt)}}{\alpha^{(wt)}}\right)\left(Z - \left(1 - \frac{C_I\gamma f_I^{(wt)}}{\alpha^{(wt)}}\right)\right)}{\beta\left(1 - \frac{\alpha^{(mut)}}{\alpha^{(wt)}}\right)} \quad (45)$$

where Z is defined as $\left(1 - \frac{\alpha^{(B)} f_I^{(wt)}}{\alpha^{(wt)}} \frac{\alpha^{(B)} f_I^{(mut)}}{\alpha^{(mut)}}\right)$ to make the equilibrium point biologically meaningful.

3.2. Analysis of the Disease-Free equilibrium Point

The system's behavior close to the equilibrium points was determined through linear stability analysis and bifurcations. It was carried out by calculation of the Jacobian matrix of the model in equilibrium points. The Jacobian matrix for eqs. (1) to (7) is given by the equation A1 in the appendix.

The disease-free equilibrium of the model is the steady-state solution of the model in the absence of the disease. The eigenvalues of the Jacobian matrix A1 at this point were calculated as follows:

$$\lambda_1 = 0 \quad (46)$$

$$\lambda_2 = -\left(\alpha^{(B)} - \gamma\right) \quad (47)$$

$$\lambda_3 = -\left(\alpha^{(B)} - \beta\right) \quad (48)$$

$$\lambda_4 = -\gamma\left(f_I^{(wt)} - \frac{\alpha^{(wt)}}{\alpha^{(B)}}\right) \quad (49)$$

$$\lambda_5 = -\gamma\left(f_I^{(mut)} - \frac{\alpha^{(mut)}}{\alpha^{(B)}}\right) \quad (50)$$

$$\lambda_6 = -\beta\left(1 - \frac{\alpha^{(wt)}}{\alpha^{(B)}}\right) \quad (51)$$

$$\lambda_7 = -\beta\left(1 - \frac{\alpha^{(mut)}}{\alpha^{(B)}}\right) \quad (52)$$

in which it is assumed that $\alpha^{(wt)} < \alpha^{(B)}$ and $\alpha^{(mut)} < \alpha^{(B)}$. Based on the general compartmental model describing an infectious disease transmission within a heterogeneous population, the host population is grouped in two general classes, the infected and uninfected compartments. Therefore, the system eqs. (1) to (7) is divided into two infected and uninfected compartments.

In classical epidemic models, it is common to observe that a disease-free equilibrium loses its stability for $\mathcal{R}_0 = 1$, and a transcritical bifurcation occurs. A transcritical bifurcation is when a fixed

Preprints (www.preprints.org) | NOT PEER-REVIEWED | Posted: 19 October 2020 doi:10.20944/preprints202010.0386.v1

point exists for all parameter values and is never destroyed. However, as the parameter values vary, such fixed point transitions from a stability region to an instability region. Biologically speaking about transcritical bifurcation: as $\mathcal{R}_0 < 1$, the disease-free equilibrium would stay stable. Thus only the commensal bacteria persist, and wild-type and mutant *Yersinia* strains cannot pass the invasion boundary. Therefore, as $\mathcal{R}_0$ increases, wild-type and mutant *Yersinia* strains, fed by commensal bacteria, can appear. We mathematically analyze this aspect within the structure of the model to assess which parts of the structure might be responsible for the occurrence of the transcritical bifurcation.

Let us consider system eqs. (1) to (7) with the above-calculated eigenvalues. Using the eigenvectors A10 shown in the appendix as a basis for a new coordinate system, we set the transformation matrix whose columns are the eigenvectors; $T = [v_1, v_2, v_3, v_4, v_5, v_6, v_7]^t$. We thus have

$$\begin{pmatrix} B_M \\ Y_M^{(wt)} \\ Y_M^{(mut)} \\ B_L \\ Y_L^{(wt)} \\ Y_L^{(mut)} \end{pmatrix} = \begin{pmatrix} \\ T \\ \\ \end{pmatrix} \begin{pmatrix} u_1 \\ u_2 \\ u_3 \\ u_4 \\ u_5 \\ u_6 \\ u_7 \end{pmatrix} \quad \text{and} \quad \begin{pmatrix} u_1 \\ u_2 \\ u_3 \\ u_4 \\ u_5 \\ u_6 \\ u_7 \end{pmatrix} = \begin{pmatrix} \\ T^{-1} \\ \\ \end{pmatrix} \begin{pmatrix} B_M \\ Y_M^{(wt)} \\ Y_M^{(mut)} \\ B_L \\ Y_L^{(wt)} \\ Y_L^{(mut)} \end{pmatrix}.$$

Under this transformation, the system eqs. (1) to (7) changes to

$$\begin{pmatrix} \dot{u}_1 \\ \dot{u}_2 \\ \dot{u}_3 \\ \dot{u}_4 \\ \dot{u}_5 \\ \dot{u}_6 \\ \dot{u}_7 \end{pmatrix} = (A) \begin{pmatrix} u_1 \\ u_2 \\ u_3 \\ u_4 \\ u_5 \\ u_6 \\ u_7 \end{pmatrix} + \begin{pmatrix} f_1(u_1, \ldots, u_7) \\ f_2(u_1, \ldots, u_7) \\ f_3(u_1, \ldots, u_7) \\ f_4(u_1, \ldots, u_7) \\ f_5(u_1, \ldots, u_7) \\ f_6(u_1, \ldots, u_7) \\ f_7(u_1, \ldots, u_7) \end{pmatrix} \tag{53}$$

where

$$A = \begin{pmatrix} 0 & 0 & 0 & 0 & 0 & 0 & 0 \\ 0 & -\frac{\gamma\left(\alpha^{(B)} f_I{}^{(wt)} - \alpha^{(wt)}\right)}{\alpha^{(B)}} & 0 & 0 & 0 & 0 & 0 \\ 0 & 0 & -\frac{\gamma\left(\alpha^{(B)} f_I{}^{(mut)} - \alpha^{(mut)}\right)}{\alpha^{(B)}} & 0 & 0 & 0 & 0 \\ 0 & 0 & 0 & -\frac{\beta\left(\alpha^{(B)} - \alpha^{(wt)}\right)}{\alpha^{(B)}} & 0 & 0 & 0 \\ 0 & 0 & 0 & 0 & -\frac{\beta\left(\alpha^{(B)} - \alpha^{(mut)}\right)}{\alpha^{(B)}} & 0 & 0 \\ 0 & 0 & 0 & 0 & 0 & -\alpha^{(B)} + \beta & 0 \\ 0 & 0 & 0 & 0 & 0 & 0 & -\alpha^{(B)} + \gamma \end{pmatrix}$$

so that the linear part is now in a standard (diagonal) form. In the $(u_1, u_2, u_3, u_4, u_5, u_6, u_7)$ coordinates, the center manifold is a curve tangent to the $u_1 -$ axis. The projection of the system onto the $u_1 -$ axis is obtained by setting $u_2 = u_3 = u_4 = u_5 = u_6 = u_7 = 0$ in the equation for $\dot{u}_1$. It yields $\dot{u}_1 = 0$.

Preprints (www.preprints.org) | NOT PEER-REVIEWED | Posted: 19 October 2020 doi:10.20944/preprints202010.0386.v1

Since E^c is one dimension, we can approximate $h_i(u_1)$ by Taylor expansion such that $u_i = h_i(u_1)$, $i \in \{2, \ldots, 7\}$, satisfy in the following equations

$$\begin{aligned} \dot{u}_2 &= Dh_2(u_1)\dot{u}_1, \\ \dot{u}_3 &= Dh_3(u_1)\dot{u}_1, \\ \dot{u}_4 &= Dh_4(u_1)\dot{u}_1, \\ \dot{u}_5 &= Dh_5(u_1)\dot{u}_1, \\ \dot{u}_6 &= Dh_6(u_1)\dot{u}_1, \\ \dot{u}_7 &= Dh_7(u_1)\dot{u}_1, \\ h_i(0) &= Dh_i(0) = 0 \end{aligned} \tag{54}$$

Thus, the reduced system is

$$\dot{u}_1 = -\frac{\alpha^{(B)}}{C_M}\, u_1^2 + \mathcal{O}\left(u_1^3\right). \tag{55}$$

The advantages of a center manifold are clear from this calculation. We may study a one-dimensional system instead of a seven-dimensional system. That is, the method of center manifolds enables one to reduce the dimension of the system by studying the flow restricted to the center manifold, in which the transients associated with the nonzero eigenvalues have decayed. As long as $\alpha^{(wt)} < \alpha^{(B)}$ and $\alpha^{(mut)} < \alpha^{(B)}$, the disease-free equilibrium point will persist. When the infection rate of wild-type and mutant strains increases, the system becomes unstable at the disease-free equilibrium point, and the trajectory of the system approaches asymptotically to the bacterial population of wild-type or mutant and finally, to the co-existence of the strains.

3.3. Computing and analysis of the system through the Basic Reproduction Number

For scenarios where multiple strains (subtypes) of an infectious disease exist, an R_0 number is calculated for each strain. Hence, in our model, we must define two different R_0, one for the wild-type and the other for the mutant strain, rather than an R_0 for the whole model. This is a significantly more difficult task. Herein, we introduce the following variations of basic reproduction number, which are calculated by the average number of secondary infections:

1. $\mathcal{R}_0^{wt}$: the basic reproductive numbers for wild-type strain = $\dfrac{\alpha^{(wt)}}{\alpha^{(B)} f_I^{(wt)}}$
2. $\mathcal{R}_0^{mut}$: the basic reproductive numbers for mutant strain = $\dfrac{\alpha^{(mut)}}{\alpha^{(B)} f_I^{(mut)}}$.

To understand the role of basic reproduction number, we also define a single reproduction number for commensal bacteria $\mathcal{R}_0^{com}$ computed as an expected number of a secondary case of commensal bacteria produced by a single commensal bacteria:

$$\mathcal{R}_0^{com} = \max\left\{\frac{\alpha^{(B)}}{\beta}, \frac{\alpha^{(B)}}{\gamma}\right\}. \tag{56}$$

Due to biologically meaningful of disease-free state P^0 and holding the conditions $\beta < \alpha^{(B)}$ and $\gamma < \alpha^{(B)}$, the disease-free state would be meaningful if $\mathcal{R}_0^{com} > 1$. Therefore, the commensal bacteria appear, $\mathcal{R}_0^{com}$ slightly reaches above one, and a stable disease-free state happens. Due to the presence of commensal bacteria and instability of the trivial solution, the solution corresponds to the extinction of all populations never appear because if $\mathcal{R}_0^{com} < 1$, all components of disease-free equilibrium will lie out of biologically meaningful region.

For $\mathcal{R}_0^{wt} < 1$ and $\mathcal{R}_0^{mut} < 1$, thus, $\lambda_1 = 0$ is a simple zero eigenvalue, and the other eigenvalues are real and negative. This implies that the transcritical bifurcation occurs in the disease-free equilibrium for $\mathcal{R}_0^{wt} < 1$ and $\mathcal{R}_0^{mut} < 1$, and the uninfected state is stable (not asymptotically stable) as none of the

Preprints (www.preprints.org) | NOT PEER-REVIEWED | Posted: 19 October 2020 doi:10.20944/preprints202010.0386.v1

strains persist. As soon as the two equilibria collide non-destructively, exchanging their stability and resulting in the Jacobian matrix having a single eigenvalue that is equal to zero, then either the mutant strain or the wild-type appears and persists for $\mathcal{R}_0^{mut}$ or $\mathcal{R}_0^{wt}$, respectively.

As shown in fig. 1, when the disease-free equilibrium loses its stability, different scenarios can occur. Herein, we discuss the different cases:

(I) If $\mathcal{R}_0^{wt} = 1$ and $\mathcal{R}_0^{mut} = 1$, then $\alpha^{(wt)} = \alpha^{(B)} f_I^{(wt)}$ and $\alpha^{(mut)} = \alpha^{(B)} f_I^{(mut)}$. Thus, the intersection of the transcritical curves $\mathcal{R}_0^{wt}$ and $\mathcal{R}_0^{mut}$ results in a triple transcritical bifurcation. As shown in A10, the Jacobian has a triple zero eigenvalue at this point ($\lambda_2 = 0, \lambda_3 = 0$). Kuznetsov has proved that such a point would be an indicator of the onset of a non-degenerate or degenerate Bogdanov–Takens bifurcation [29,30]. The disease-free equilibrium P^0 is loosing its stability and the wild-type-free and mutant-free are including one simple zero eigenvalue ($\lambda_3 = 0$), meaning that the dynamic of the model are changing as the target parameter is in the threshold value.

(II) If $\mathcal{R}_0^{wt} > 1$, the wild-type strain equilibrium in the region II will persist when $\mathcal{R}_0^{mut} < 1$. The wild-type strain will spread and possibly persist within the host population. In general, for a strain to persist, its basic reproduction number has to be strictly greater than one. Therefore, in this region, the disease-free, mutant strain and co-existence state exchange stability: P^0 becomes unstable, P^2 becomes locally asymptotically stable, and P^1 and P^3 remain unstable. This means that the immune system could kill one of the strains more efficiently.

(III) If $\mathcal{R}_0^{mut} > 1$, the mutant strain equilibrium in the region III will persist when $\mathcal{R}_0^{wt} < 1$. The mutant strain will spread and possibly persist within the host population since its basic reproduction number is greater than one. Therefore, in this region, the disease-free, wild-type strain, and co-existence state exchange stability: P^0 becomes unstable, P^1 becomes locally asymptotically stable, and P^2 and P^3 remain unstable. This means that the immune system could defeat the wild-type strains. However, the risk of happening this situation is low because the **mutant!** strains are influenced more efficiently than wild-type strains by immune action.

(IV) If $\mathcal{R}_0^{wt} > 1$ and $\mathcal{R}_0^{mut} > 1$, the co-existence population spreads, and both strains persist. The Overall $\mathcal{R}_0$ can be defined as $\mathcal{R}_0^c = d\,\mathcal{R}_0^{mut} + (1-d)\,\mathcal{R}_0^{wt}$. A mutant with $d = 1$ is thoroughly dominant, while one with $d = 0$ is completely recessive; scenarios of incomplete dominance $(0 < d < 1)$, under-dominance $(d < 0)$, and over-dominance $(d > 1)$ are possible as well. For instance, a mutant could achieve a higher $\mathcal{R}_0$ than the wild-type via a higher growth rate that increases transmission. In a co-infection, the faster-growing mutant strain would outcompete the wild-type and reach its maximum capacity. This situation would change the co-infection to the conditions where a single infection happens. Thus, the overall $\mathcal{R}_0$ of the co-infection would be similar to that of the mutant by itself, making the mutant a dominant one. Furthermore, the effort for having co-existence equilibrium and analysis of the co-infection model will fail. By contrast, let us assume a mutant strain achieves a higher $\mathcal{R}_0$. Nevertheless, the virulence of the wild-type strain neutralizes the higher $\mathcal{R}_0$ value of the mutant. This would make the mutant a recessive one. In summary, virtually any two-strain co-infection model can be mapped to a set of values for d, allowing scenarios of particular interest to be explored in a context broader than the one possible with typical models.

The mathematical model eqs. (1) to (7) calculates the number of pathogen-specific characteristics in different layouts, e.g., when colonization resistance mediated by the endogenous microbiome is lacking or when the immune response is partially impaired. In this paper, we use the experimental data obtained in the lab upon infection of a host either lacking a microbiome (mimicking antibiotic treatment of patients) or a fully functional immune system [10].

To challenge the numerical simulation with experimental data, we tested whether the numerical simulation from the mathematical analysis could fit the experimental data.

Correspondingly, we simulated the process of *Yersinia enterocolitica* co-infection in specific-pathogen-free (SPF) (i.e., wild-type), germ-free (GF), and MyD88-deficient mice (MyD88$^{-/-}$) mutant mice. Using the model values in table 3, which was estimated through experimental data [10],

Preprints (www.preprints.org) | NOT PEER-REVIEWED | Posted: 19 October 2020 doi:10.20944/preprints202010.0386.v1

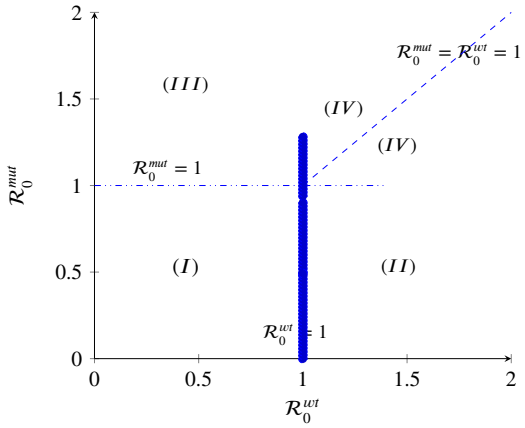

Figure 1. The diagram displaying three regions with different qualitative behaviors in terms of the basic reproduction numbers. Region I: Infection-free state; Region II: mutant-free state; Region III: wild-type-free state; and Region IV: co-existence of all strains.

we first examined the influence of the infection rates $\alpha^{(B)}$, $\alpha^{(wt)}$, and $\alpha^{(mut)}$ on the dynamics beginning by constructing one-dimensional bifurcation diagrams using $\alpha^{(B)}$ as the bifurcation parameter and fixing $\alpha^{(wt)}$ and $\alpha^{(mut)}$.

Table 3. Parameter values

Parameter	Values in Ye SPF wt/A0	Values in Ye SPF wt/T3S0	Values in Ye GF wt/A0	Values in Ye MyD88$^{-/-}$ wt/A0
$\alpha^{(B)}$	$4.89 \cdot 10^{-1}$	2.00	1.99	$5.40 \cdot 10^{-1}$
$\alpha^{(wt)}$	$4.44 \cdot 10^{-1}$	1.86	1.60	$5.78 \cdot 10^{-1}$
$\alpha^{(mut)}$	$4.44 \cdot 10^{-1}$	1.86	1.60	$5.78 \cdot 10^{-1}$
$f_I^{(wt)}$	$3.96 \cdot 10^{-1}$	$9.48 \cdot 10^{-3}$	$1.10 \cdot 10^{-1}$	$6.23 \cdot 10^{-2}$
$f_I^{(mut)}$	$1.95 \cdot 10^{-1}$	$3.73 \cdot 10^{-1}$	$1.19 \cdot 10^{-1}$	$1.28 \cdot 10^{-1}$
C_M	$1.76 \cdot 10^{5}$	$6.27 \cdot 10^{3}$	$1.3 \cdot 10^{6}$	$1.28 \cdot 10^{5}$
C_L	$2.14 \cdot 10^{7}$	$6.13 \cdot 10^{6}$	$4.99 \cdot 10^{9}$	$9.98 \cdot 10^{9}$
C_I	1.00	1.00	1.00	1.00
γ	1.00	1.00	$9.97 \cdot 10^{-1}$	$1.00 \cdot 10^{-1}$
κ	$7.83 \cdot 10^{-1}$	$4.28 \cdot 10^{-1}$	$6.50 \cdot 10^{-1}$	$4.37 \cdot 10^{-1}$
β	$2.50 \cdot 10^{-1}$	$2.50 \cdot 10^{-1}$	$8.33 \cdot 10^{-2}$	$1.82 \cdot 10^{-1}$

As shown in fig. 2, $\mathcal{R}_0^{com}$ should be larger than one to achieve the disease-free equilibrium. As long as, $\mathcal{R}_0^{wt}$ and $\mathcal{R}_0^{mut}$ are smaller than one. The disease-free equilibrium is stable.

Following the analysis of the model in respect to $\alpha^{(B)}$, two cases are considered. The first case is when $\alpha^{(wt)}$ and $\alpha^{(mut)}$ are equal. In this case, we do not have co-existence of wild-type and mutant (the denominator of $Y_L^{3(wt)}$ and $Y_L^{3(mut)}$ will be equal to zero). The second one is when $\alpha^{(wt)}$ and $\alpha^{(mut)}$ have different values as the co-existence equilibrium is achieved and be biologically meaningful.

Thus, we start with values of the wt and mut-strain infections rate given by $\alpha^{(wt)} = 4.44 \cdot 10^{-1}$ and $\alpha^{(wt)} = 4.44 \cdot 10^{-1}$ of table 3. Corresponding to those infections rates, the basic reproduction numbers $\mathcal{R}_0{}^{(wt)}$ and $\mathcal{R}_0{}^{(mut)}$ in terms of $\alpha^{(B)}$ are computed.

Through the definition of $\mathcal{R}_0^{com}$, $\mathcal{R}_0^{wt}$ and $\mathcal{R}_0^{mut}$, we display a x-scale as $\alpha^{(B)}$ fig. 3. This shows the appearance of different equilibrium of model eq. (14) in terms of the basic reproduction numbers.

As shown in fig. 3, we expect no co-existence equilibrium when $\alpha^{(wt)} = \alpha^{(mut)}$ and only wild-type equilibrium exists (mutant-free equilibrium) when $1.76 < \alpha^{(B)} < 11.20$. However, the disease-free equilibrium can happen when $\alpha^{(B)}$ is large enough to surpass $\alpha^{(wt)}$ and $\alpha^{(mut)}$. These findings are displayed in fig. 4.

Secondly, to show the appearance of the co-existence, we consider the parameter values of in Ye wt/T3S0 table 3 with assumption of $1.86 = \alpha^{wt} \neq \alpha^{mut} = 1.83$. Thus we compute $\mathcal{R}_0^{wt}$ and $\mathcal{R}_0^{mut}$

Preprints (www.preprints.org) | NOT PEER-REVIEWED | Posted: 19 October 2020 doi:10.20944/preprints202010.0386.v1

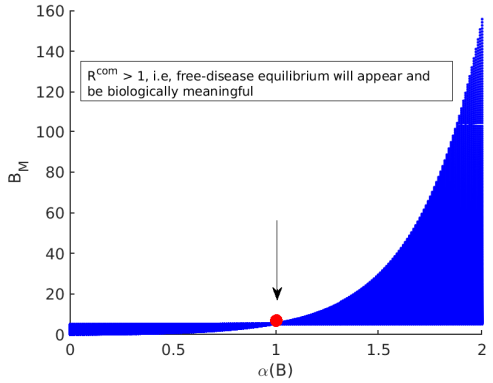

(a) Biologically meaningful region for commensal bacteria in the mucosa

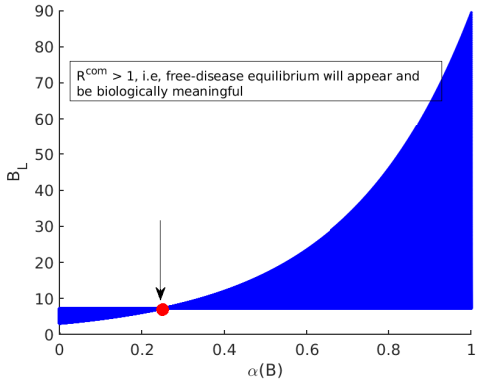

(b) Biologically meaningful region for commensal bacteria in the lumen

Figure 2. The diagram displaying the role $\mathcal{R}_0^{com}$ in appearance/non-appearance of trivial solution and disease-free equilibrium. a By fixing the parameter values table 3 in model eq. (14), the commensal bacteria in the mucosa appear when $\mathcal{R}_0^{com} > 1$. Therefore, as long as $\mathcal{R}_0^{com} < 1$, only trivial solution for the model exist. Since the trivial solution is always unstable, the extinction of all populations never achieved. b By fixing the parameter values table 3 in model eq. (14), the commensal bacteria in the lumen appear when $\mathcal{R}_0^{com} > 1$. Therefore, as long as $\mathcal{R}_0^{com} < 1$, only trivial solution for the model exist. Since the trivial solution is always unstable, the extinction of all populations never achieved.

in respect to parameter $\alpha^{(B)}$. This results in appearance co-existence when $1 < \alpha^{(B)} < 4.90$ as fig. 5 shows.

Furthermore, we analyze the immune system's influence. In our model, at least one Ye within the mucosal compartment activates the immune system. This activation increases proportionally to the number of Ye. The immune system is assumed to influence the bacterial populations primarily at the mucosal site compared to bacteria within the lumen. Herein, we simulate the process of *Yersinia enterocolitica* with an immune response that was experienced on SPF, GF, and MyD88$^{-/-}$ mice. As the response of the immune system in these mice are different, so we conclude different behavior. Let us denote the numerical simulation:

- The effect of maximum rate of immune growth κ on wild-type *Yersinia* strain in the mucosa fig. 6,
- The effect of maximum rate of immune growth κ on mutant *Yersinia* strain in the mucosa fig. 7,
- The effect of maximum rate of immune growth κ on wild-type *Yersinia* strain in the lumen fig. 8,
- The effect of maximum rate of immune growth κ on mutant *Yersinia* strain in the lumen fig. 9,

The experimental data obtained in the lab has been shown that the Ye mutant strain is eliminated more efficiently than Ye wt at a mucosal compartment. However, since GF mice lack a microbiome, both the Ye wt and the mutant strain can colonize the gastrointestinal tract (GIT) at high numbers. In the SPF-colonized **Myd88!** (**Myd88!**) mice, the immune response is weaker [10]. Therefore, as shown in fig. 6, fig. 7, fig. 8, and fig. 9, the following results conclude:

- fig. 6d and fig. 7d shows a slow reduction of the wt strain in compare with mut strain as κ is changing.
- fig. 6b, fig. 7b, fig. 8b, and fig. 9b in compare with similar situations in SPF and MyD88$^{-/-}$ shows elimination of wt and mut strains in less efficient.
- fig. 6c, fig. 7c, fig. 8c and fig. 9c shows that wt and the mutant strains increased faster. Besides. the influence κ on wt and the mutant strains can not project properly (fig. 8f, fig. 9f) in a same speed of producing strains.

Our results allow us to state that if mice possess a healthy microbiota and immune system, as long as the growth rate of commensal bacteria is larger than the growth rate of wild-type and mutant *Yersinia*, then the infection will not spread as Ye strains cannot enter the lumen compartment. Therefore,

Preprints (www.preprints.org) | NOT PEER-REVIEWED | Posted: 19 October 2020 doi:10.20944/preprints202010.0386.v1

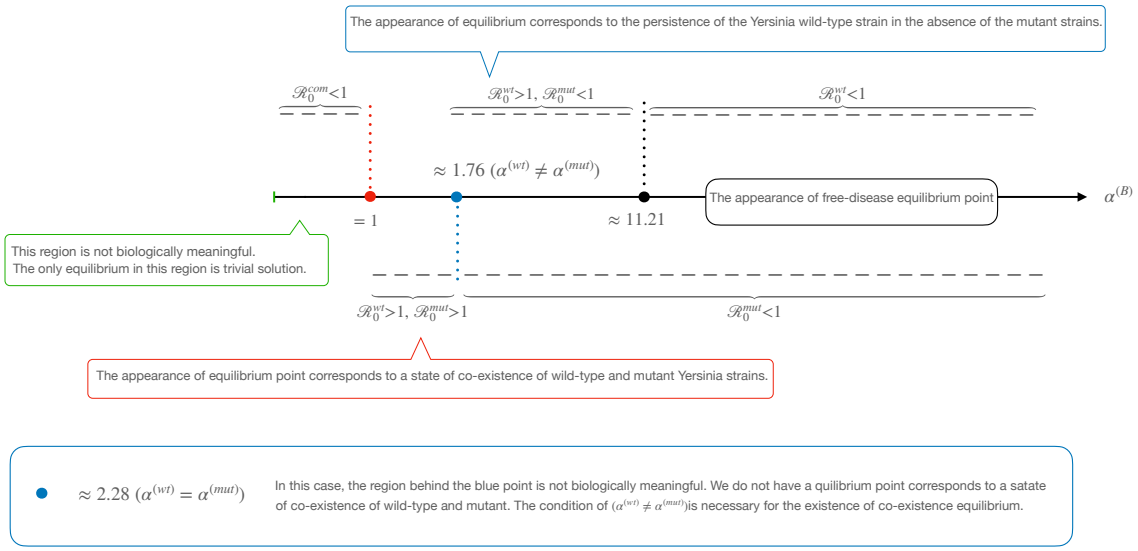

Figure 3. The diagram displaying $\alpha^{(B)}$ regions with appearance of different equilibrium in terms of the basic reproduction numbers. This displays is plotted by fixing the parameter values table 3 in model eq. (14).

the disease-free equilibrium, P^0 exists and is stable when $\mathcal{R}_0^{wt}$ and $\mathcal{R}_0^{mut}$ are less than one while $\alpha^{(B)}$ is large enough. To challenge this situation, we test the data values Ye SPF wt/A0 table 3 with the assumed boundary $\alpha^{(B)} > 11.20$ to face a disease-free state fig. 3. Our computer simulations run for 366 hours and are shown in fig. 10. As predicted for disease-free state, the commensal fraction B_M and B_L approach their carrying capacity C_M and C_L, respectively.

Therefore, we noted that the disease-free equilibrium always exists and is (asymptotically) stable whenever the reproductive numbers for both strains of the disease were below unity. Simulations support these findings. The two single-strain equilibria, where one strain persists while the other strain dies out, are symmetrical and exist when at least one of the strains has a reproductive number above the unity. However, in our model eq. (14) with parameter values table 3, we could not observe a state that corresponds to Ye mut strain equilibrium. As shown in fig. 3, there is no region where $\mathcal{R}_0^{mut} > 1$ and $\mathcal{R}_0^{wt} < 1$. Whenever $\mathcal{R}_0^{mut} > 1$, $\mathcal{R}_0^{wt}$ is already above one; this facilitates the situation for a co-existence equilibrium. This is where both strains persist, exists when both reproductive numbers are above a certain threshold. However, we could not analytically solve stability criteria for the equilibrium due to complexity, but simulations show that this stability criteria exist.

4. Discussion and Conclusions

In this paper, we proved that our computational model of the *Yersinia enterocolitica* [10] population in co-infections of mice with Ye wt and mut strains always have stability results in terms of $\mathcal{R}_0$, such that if we can keep or reduce $\mathcal{R}_0$s to less than one, then wild-type and mutant strains can not spread, and the infection resolves. We predicted medical control strategies for this infectious disease through the basic reproduction number. Furthermore, we analyzed at which level of sensibility, the system's parameters change the model's invasion behavior. Besides, we looked for conditions in the immune system to see a different scenario of a weaker and stronger immune system in fighting against infection. We found that immunity alone never creates a backward bifurcation of the disease-free steady state under biologically realistic hypotheses. This did not rule out the possibility of stable equilibria, but we provided some other sufficient conditions for the uniqueness of the multiple equilibria. Our results indicate that the within-host dynamics of immunity can, in principle, have important consequences for

Preprints (www.preprints.org) | NOT PEER-REVIEWED | Posted: 19 October 2020 doi:10.20944/preprints202010.0386.v1

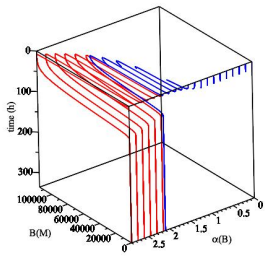

(a) Commensals in the mucosa concerning $\alpha^{(B)}$

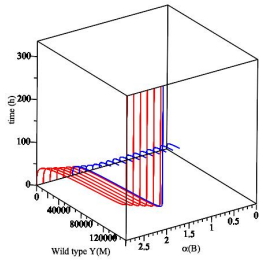

(b) Wild-type *Yersinia* in the mucosa concerning $\alpha^{(B)}$

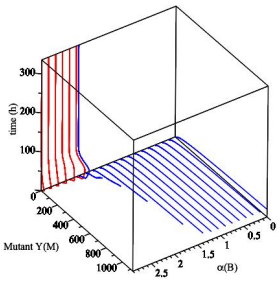

(c) Mutant *Yersinia* in the mucosa concerning $\alpha^{(B)}$

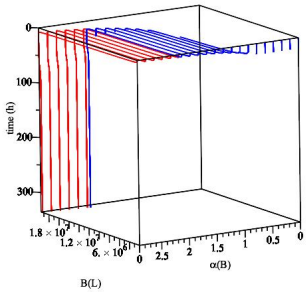

(d) Commensals in the lumen concerning $\alpha^{(B)}$

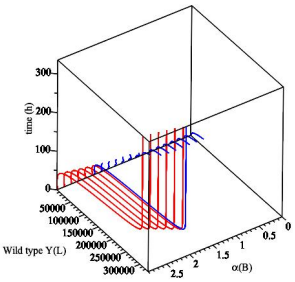

(e) Wild-type *Yersinia* in the lumen concerning $\alpha^{(B)}$

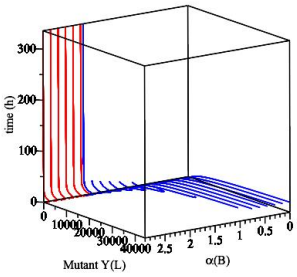

(f) Mutant *Yersinia* in the lumen concerning $\alpha^{(B)}$

Figure 4. The sensitivity of parameter in respect to $\alpha^{(B)}$ for 336 hours. $0 < \alpha^{(B)} < 1$, no biologically meaningful region (out of our interest). $\alpha^{(B)} > 1$, all populations appear. When $1 < \alpha^{(B)} < 2.28$, the region is a region for the appearance of the co-existence equilibrium, but the hypothesis of the co-existence equilibrium is not satisfied. Therefore, wild-type strain does not grow, and the mutant strain is going down slowly. When $\alpha^{(B)} > 2.28$, this is a region of the appearance of wild-type equilibrium ($\mathcal{R}_0^{wt} > 1$). Thus, a and e are increasing fast and staying in the maximum level as a and d are going back to zero. Additionally, c and d do not grow anymore ($\mathcal{R}_0^{mut} < 1$).

population-level dynamics, but also suggest that this would require strong non-monotone effects in the immune response to infection.

Furthermore, this also raises the question of whether the infection becomes persistent or is resolved. The answer to this question depends on the magnitude of the basic reproductive number, $\mathcal{R}_0$, since the calculation of the stability of equilibrium is very complicated. As shown, the disease-free equilibrium is locally (asymptotically) stable when $0 < \mathcal{R}_0 < 1$ and unstable if $\mathcal{R}_0 > 1$. In other words, when $0 < \mathcal{R}_0 < 1$, every infectious strain will cause less than one secondary infection, and hence the disease will die. When $\mathcal{R}_0 > 1$, every infectious strain will cause more than one secondary infection, and hence *Yersinia* infection will occur. All public health control measures can usually be based on methods that, if practical, would lower $\mathcal{R}_0$ to below unity. On the other hand, the co-infection equilibrium is locally stable when $\mathcal{R}_0 > 1$ and unstable when $0 < \mathcal{R}_0 < 1$. Typically, for Ye, we do not observe the spread of infection. However, Ye is a great model system and can be used to predict the spread of infections by more clinically relevant bugs, e.g., enteropathogenic or enterohemorrhagic *Escherichia coli*. To control the spread of infection, efforts must be made to ensure that the co-infection equilibrium is unstable, i.e., $0 < \mathcal{R}_0 < 1$.

In a co-infection setup, we found two thresholds for the model, $\mathcal{R}_0^{wt}$ and $\mathcal{R}_0^{mut}$. The threshold associated with the wild-type and mutant strains determine the existence and the stability of the equilibrium point, and we considered four equilibrium points for the model.

As the theoretical work agrees with the experimental work, our results may be used to control the spread of infection by other pathogens of the gastrointestinal tract, e.g., enteropathogenic or

Preprints (www.preprints.org) | NOT PEER-REVIEWED | Posted: 19 October 2020 doi:10.20944/preprints202010.0386.v1

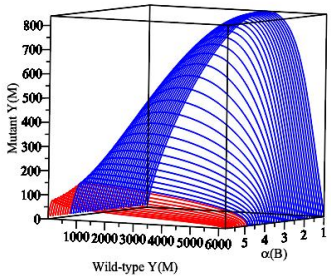

(a) Co-existence of wild-type and mutant *Yersinia* strains in the mucosa

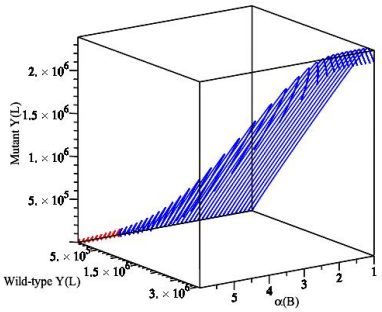

(b) Co-existence of wild-type and mutant *Yersinia* strains in the lumen

Figure 5. The diagram displays the appearance of the co-existence of wild-type and mutant *Yersinia* strains as $\alpha^{(B)}$ is changing in a region where $\mathcal{R}_0^{wt} > 1$ and $\mathcal{R}_0^{mut} > 1$. a An immune reaction influences the wild-type and mutant *Yersinia* strains in the mucosa. Additionally, another part of them is spilled over and move to the lumen compartment. Therefore, they are simultaneously increasing to reach their maximum values and decreasing. b The wild-type and mutant *Yersinia* strains in the lumen are simultaneously increasing to reach the carrying capacity of the lumen compartment. In both a and b, when $\alpha^{(B)}$ is reaching 4.90, the co-existence of wild-type and mutant *Yersinia* strains is disappearing.

enterohemorrhagic *E. coli*. Furthermore, an additional factor to take into account is whether antibiotics are used from the beginning of the infection, in which case the spread of *Yersinia* might have been extinguished or not. We also believe that further research into the elaborate makeup of the strains and on how the immune system differentiates between strains could be incorporated to more accurately represent control policy.

Author Contributions: Conceptualization, R.M., M.E., and A.D.; methodology, R.M.; software, R.M.; validation, R.M., A.D., and M.E.; formal analysis, R.M.; investigation, A.D.; resources, A.D.; data curation, R.M. and A.D.; writing–original draft preparation, R.M.; writing–review and editing, A.D.; visualization, R.M.; supervision, A.D.; project administration, A.D.; funding acquisition, R.M. and A.D.

Funding: This research was funded by the German Center for Infection Research (DZIF, doi: 10.13039/100009139) within the *Deutsche Zentren der Gesundheitsforschung* (BMBF-DZG, German Centers for Health Research of the Federal Ministery of Education and Research), grant № 8020708703 and supported by infrastructural funding from the *Deutsche Forschungsgemeinschaft* (DFG, German Research Foundation), Cluster of Excellence EXC 2124 Controlling Microbes to Fight Infections.

Acknowledgments: The authors thank Libera Lo Presti for feedback on this manuscript.

Conflicts of Interest: The authors declare no conflict of interest.

Abbreviations

AMP	anti-microbial peptide
BMBF-DZG	*Deutsche Zentren der Gesundheitsforschung*
CFU	colony-forming unit
DFE	disease-free equilibrium
DFG	*Deutsche Forschungsgemeinschaft*
DZIF	German Center for Infection Research
GF	germ-free
GIT	gastrointestinal tract
mut	mutant
MyD88$^{-/-}$	MyD88-deficient mice
ODE	Ordinary Differential Equation
RKI	Robert Koch Institute
SI	small intestine
SPF	specific-pathogen-free
T3SS	Type III secretion system

Preprints (www.preprints.org) | NOT PEER-REVIEWED | Posted: 19 October 2020 doi:10.20944/preprints202010.0386.v1

wt	wild-type
YadA	Yersinia adhesin A
Ye	*Yersinia entercolitica*
Yop	*Yersinia* outer protein

Appendix A. Mathematical Calculation

Appendix A.1. Jacobian

The Jacobian of the system eqs. (1) to (7) is calculated as follows:

$$J = \begin{pmatrix} \alpha^{(B)}\left(1-\frac{2B_M+Y_M^{(wt)}+Y_M^{(mut)}}{C_M}\right)-\gamma I & -\frac{\alpha^{(B)}B_M}{C_M} & 0 & 0 & 0 & 0 \\ -\frac{\alpha^{(wt)}Y_M^{(wt)}}{C_M} & \alpha^{(wt)}\left(1-\frac{B_M+2Y_M^{(wt)}+Y_M^{(mut)}}{C_M}\right)-\gamma I f_I^{(wt)} & 0 & 0 & 0 & 0 \\ -\frac{\alpha^{(mut)}Y_M^{(mut)}}{C_M} & -\frac{\alpha^{(mut)}Y_M^{(mut)}}{C_M} & \alpha^{(mut)}\left(1-\frac{B_M+2Y_M^{(wt)}+Y_M^{(mut)}}{C_M}\right)-\gamma I f_I^{(mut)} & 0 & 0 & 0 \\ \alpha^{(B)}\frac{2B_M+Y_M^{(wt)}+Y_M^{(mut)}}{C_M} & \frac{\alpha^{(B)}B_M}{C_M} & \frac{\alpha^{(B)}B_M}{C_M} & \alpha^{(B)}\left(1-\frac{2B_L+Y_L^{(wt)}+Y_L^{(mut)}}{C_L}\right)-\beta & 0 & 0 \\ \frac{\alpha^{(wt)}Y_M^{(wt)}}{C_M} & \alpha^{(wt)}\frac{B_M+2Y_M^{(wt)}+Y_M^{(mut)}}{C_M} & \frac{\alpha^{(wt)}Y_M^{wt}}{C_M} & -\frac{\alpha^{(wt)}Y_L^{(wt)}}{C_L} & 0 & 0 \\ \frac{\alpha^{(mut)}Y_M^{(mut)}}{C_M} & \frac{\alpha^{(mut)}Y_M^{(mut)}}{C_M} & \alpha^{(mut)}\frac{B_M+Y_M^{(wt)}+2Y_M^{(mut)}}{C_M} & -\frac{\alpha^{(mut)}Y_L^{(mut)}}{C_L} & 0 & 0 \\ 0 & \frac{\kappa(C_I-I)}{C_I} & \frac{\kappa(C_I-I)}{C_I} & 0 & 0 & 0 \\ 0 & 0 & 0 & -\frac{\alpha^{(B)}B_L}{C_L} & -\gamma B_M & 0 \\ 0 & 0 & 0 & -\frac{\alpha^{(wt)}Y_L^{wt}}{C_L} & -\gamma f_I^{(wt)}Y_M^{(wt)} & 0 \\ 0 & 0 & 0 & \alpha^{(mut)}\left(1-\frac{B_L+Y_L^{(wt)}+2Y_L^{(mut)}}{C_L}\right)-\beta & -\gamma f_I^{(mut)}Y_M^{(mut)} & 0 \\ \alpha^{(wt)}\left(1-\frac{B_L+2Y_L^{(wt)}+Y_L^{(mut)}}{C_L}\right)-\beta & -\frac{\alpha^{(B)}B_L}{C_L} & -\frac{\alpha^{(B)}B_L}{C_L} & 0 & 0 & 0 \\ -\frac{\alpha^{(mut)}Y_L^{(mut)}}{C_L} & -\frac{\alpha^{(wt)}Y_L^{wt}}{C_L} & 0 & 0 & 0 & 0 \\ 0 & \alpha^{(mut)}\left(1-\frac{B_L+Y_L^{(wt)}+2Y_L^{(mut)}}{C_L}\right)-\beta & 0 & 0 & 0 & -\frac{\kappa(Y_M^{(wt)}+Y_M^{(mut)})}{C_I} \end{pmatrix} \tag{A1}$$

Appendix A.2. The eigenvalues of trivial equilibrium point

The eigenvalues for trivial equilibrium point are as follows:

$$\lambda_1 = 0 \tag{A2}$$

$$\lambda_2 = \alpha^{(B)} \tag{A3}$$

$$\lambda_3 = \alpha^{(wt)} \tag{A4}$$

$$\lambda_4 = \alpha^{(mut)} \tag{A5}$$

Preprints (www.preprints.org) | NOT PEER-REVIEWED | Posted: 19 October 2020 doi:10.20944/preprints202010.0386.v1

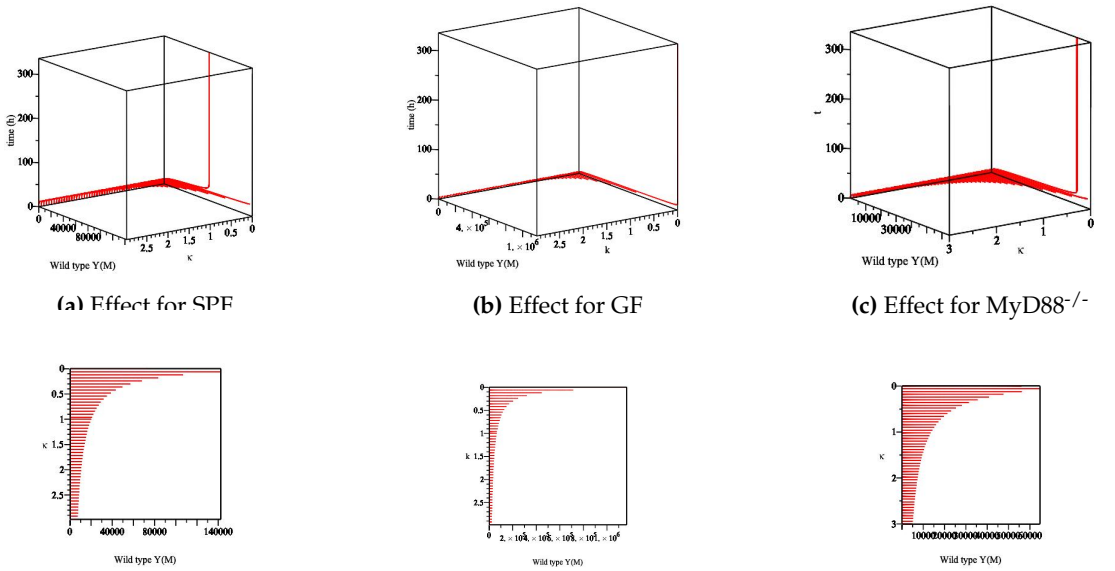

(a) Effect for SPF **(b)** Effect for GF **(c)** Effect for MyD88$^{-/-}$

(d) Projection for SPF **(e)** Projection for GF **(f)** Projection for MyD88$^{-/-}$

Figure 6. The sensitivity of parameter κ in elimination of wild-type *Yersinia* strain in the mucosa. a to c The effect of the parameter κ on the different mice. d to f The projection of κ for different mice.

$$\lambda_5 = \alpha^{(B)} - \beta \tag{A6}$$

$$\lambda_6 = \alpha^{(wt)} - \beta \tag{A7}$$

$$\lambda_7 = \alpha^{(mut)} - \beta \tag{A8}$$

$$\tag{A9}$$

Appendix A.3. The eigenvalues and eigenvectors of disease-free equilibrium point

The eigenvectors correspond to the eigenvalues for disease-free equilibrium point are as follows:

$$\lambda_1 = 0, \qquad v_1 = \left[-\frac{\gamma C_M}{\alpha^{(B)}}, 0, 0, 0, 0, 0, 1\right] \tag{A10}$$

$$\lambda_2 = -\frac{\gamma\left(f_I{}^{(wt)}\alpha^{(B)} - \alpha^{(wt)}\right)}{\alpha^{(B)}}, \qquad v_2 = [v_{21}, v_{22}, 0, 1, v_{25}, 0, v_{27}] \tag{A11}$$

$$\lambda_3 = -\frac{\gamma\left(f_I{}^{(mut)}\alpha^{(B)} - \alpha^{(mut)}\right)}{\alpha^{(B)}}, \qquad v_3 = [v_{31}, 0, v_{33}, 1, 0, v_{36}, v_{37}] \tag{A12}$$

$$\lambda_4 = -\frac{\beta\left(\alpha^{(B)} - \alpha^{(wt)}\right)}{\alpha^{(B)}}, \qquad v_4 = \left[0, 0, 0, 1, -\frac{\left(\alpha^{(B)}\right)^2 - 2\alpha^{(B)}\beta + \beta\alpha^{(wt)}}{\alpha^{(B)}\left(\alpha^{(B)} - \beta\right)}, 0, 0\right] \tag{A13}$$

$$\lambda_5 = -\frac{\beta\left(\alpha^{(B)} - \alpha^{(mut)}\right)}{\alpha^{(B)}}, \qquad v_5 = \left[0, 0, 0, 1, 0, -\frac{\left(\alpha^{(B)}\right)^2 - 2\alpha^{(B)}\beta + \beta\alpha^{(mut)}}{\alpha^{(B)}\left(\alpha^{(B)} - \beta\right)}, 0\right] \tag{A14}$$

$$\lambda_6 = -\alpha^{(B)} + \beta, \qquad v_6 = [0, 0, 0, 1, 0, 0, 0] \tag{A15}$$

$$\lambda_7 = -\alpha^{(B)} + \gamma, \qquad v_7 = [1, 0, 0, 0, 0, 0, 0] \tag{A16}$$

Preprints (www.preprints.org) | NOT PEER-REVIEWED | Posted: 19 October 2020 doi:10.20944/preprints202010.0386.v1

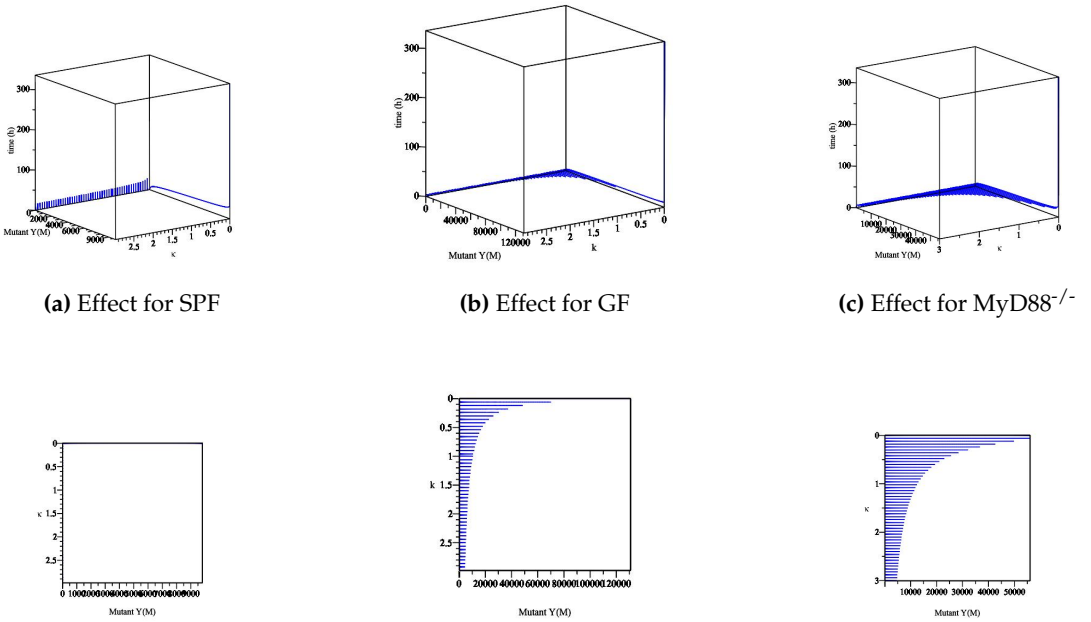

(a) Effect for SPF **(b)** Effect for GF **(c)** Effect for MyD88$^{-/-}$

(d) Projection for SPF **(e)** Projection for GF **(f)** Projection for MyD88$^{-/-}$

Figure 7. The sensitivity of parameter κ in elimination of mutant *Yersinia* strain in the mucosa.

Appendix A.4. The eigenvalues wild-type strain equilibrium

The eigenvalues of equilibrium of wild-type strain are calculated as

$$\lambda_1 = -C_I\gamma\left(f_I{}^{(mut)} - \frac{\alpha^{(mut)} f_I{}^{(wt)}}{\alpha^{(wt)}}\right) \tag{A17}$$

$$\lambda_2 = -\alpha^{(wt)}\left(1 - \frac{C_I\gamma\, f_I{}^{(wt)}}{\alpha^{(wt)}}\right) \tag{A18}$$

$$\lambda_3 = -C_I\gamma\left(1 - \frac{\alpha^{(B)} f_I{}^{(wt)}}{\alpha^{(wt)}}\right) \tag{A19}$$

$$\lambda_4 = -\frac{\kappa\, C_M}{C_I}\left(1 - \frac{C_I\gamma\, f_I{}^{(wt)}}{\alpha^{(wt)}}\right) \tag{A20}$$

$$\lambda_5 = -\alpha^{(wt)}\sqrt{4\frac{C_M}{C_L}\left(1 - \frac{C_I\gamma f_I^{(wt)}}{\alpha^{(wt)}}\right)^2 + \left(1 - \frac{\beta}{\alpha^{(wt)}}\right)^2} \tag{A21}$$

$$\lambda_6 = -\frac{1}{2}\left(2\beta - \alpha^{(B)}\left(1 + \frac{\beta}{\alpha^{(wt)}}\right) + \alpha^{(B)}\sqrt{4\frac{C_M}{C_L}\left(1 - \frac{C_I\gamma f_I^{(wt)}}{\alpha^{(wt)}}\right)^2 + \left(1 - \frac{\beta}{\alpha^{(wt)}}\right)^2}\right) \tag{A22}$$

$$\lambda_7 = -\frac{1}{2}\left(2\beta - \alpha^{(mut)}\left(1 + \frac{\beta}{\alpha^{(wt)}}\right) + \alpha^{(mut)}\sqrt{4\frac{C_M}{C_L}\left(1 - \frac{C_I\gamma f_I^{(wt)}}{\alpha^{(wt)}}\right)^2 + \left(1 - \frac{\beta}{\alpha^{(wt)}}\right)^2}\right) \tag{A23}$$

Preprints (www.preprints.org) | NOT PEER-REVIEWED | Posted: 19 October 2020 doi:10.20944/preprints202010.0386.v1

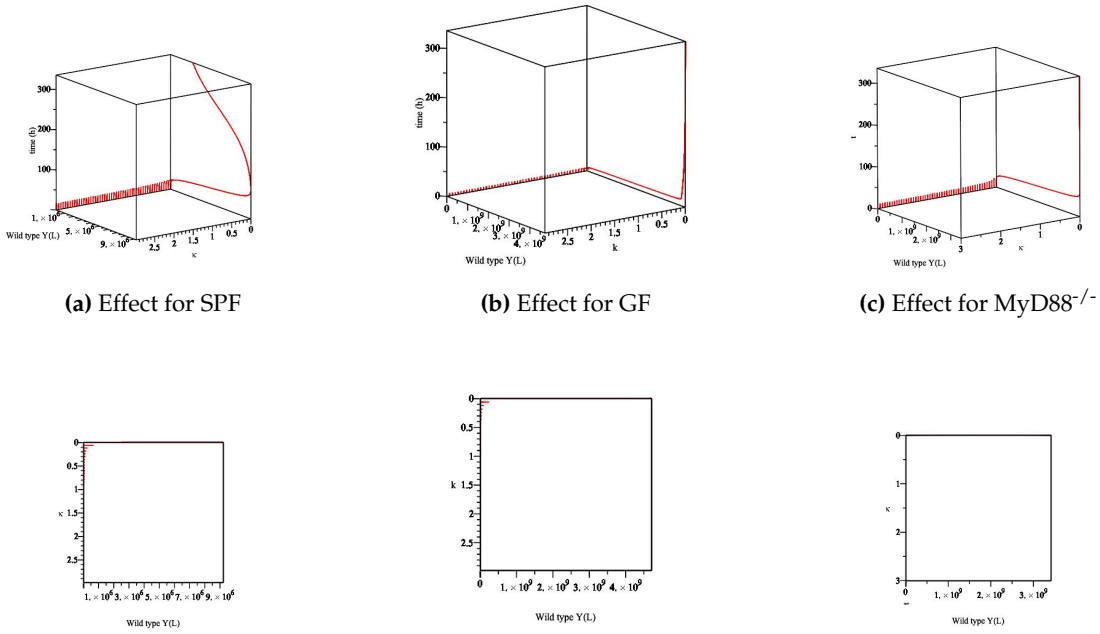

(a) Effect for SPF **(b)** Effect for GF **(c)** Effect for MyD88$^{-/-}$

(d) Projection for SPF **(e)** Projection for GF **(f)** Projection for MyD88$^{-/-}$

Figure 8. The sensitivity of parameter κ in elimination of wild-type *Yersinia* strain in the lumen

Appendix A.5. The eigenvalues mutant strain equilibrium

The eigenvalues of equilibrium of mutant strain are calculated as

$$\lambda_1 = -C_I\gamma\left(f_I{}^{(wt)} - \frac{\alpha^{(wt)}f_I{}^{(mut)}}{\alpha^{(mut)}}\right) \tag{A24}$$

$$\lambda_2 = -\alpha^{(mut)}\left(1 - \frac{C_I\gamma f_I{}^{(mut)}}{\alpha^{(mut)}}\right) \tag{A25}$$

$$\lambda_3 = -C_I\gamma\left(1 - \frac{\alpha^{(B)}f_I{}^{(mut)}}{\alpha^{(mut)}}\right) \tag{A26}$$

$$\lambda_4 = -\frac{\kappa C_M}{C_I}\left(1 - \frac{C_I\gamma f_I{}^{(mut)}}{\alpha^{(mut)}}\right) \tag{A27}$$

$$\lambda_5 = -\alpha^{(mut)}\sqrt{4\frac{C_M}{C_L}\left(1 - \frac{C_I\gamma f_I^{(mut)}}{\alpha^{(mut)}}\right)^2 + \left(1 - \frac{\beta}{\alpha^{(mut)}}\right)^2} \tag{A28}$$

$$\lambda_6 = -\frac{1}{2}\left(2\beta - \alpha^{(B)}\left(1 + \frac{\beta}{\alpha^{(mut)}}\right) + \alpha^{(B)}\sqrt{4\frac{C_M}{C_L}\left(1 - \frac{C_I\gamma f_I^{(mut)}}{\alpha^{(mut)}}\right)^2 + \left(1 - \frac{\beta}{\alpha^{(mut)}}\right)^2}\right) \tag{A29}$$

$$\lambda_7 = -\frac{1}{2}\left(2\beta - \alpha^{(wt)}\left(1 + \frac{\beta}{\alpha^{(mut)}}\right) + \alpha^{(wt)}\sqrt{4\frac{C_M}{C_L}\left(1 - \frac{C_I\gamma f_I^{(mut)}}{\alpha^{(mut)}}\right)^2 + \left(1 - \frac{\beta}{\alpha^{(mut)}}\right)^2}\right) \tag{A30}$$

Appendix A.6. The basic reproduction numbers

The calculation of the basic reproduction number is as follows:

1. We consider the first four equations corresponds to the infected compartment from eqs. (22) to (28)

Preprints (www.preprints.org) | NOT PEER-REVIEWED | Posted: 19 October 2020 doi:10.20944/preprints202010.0386.v1

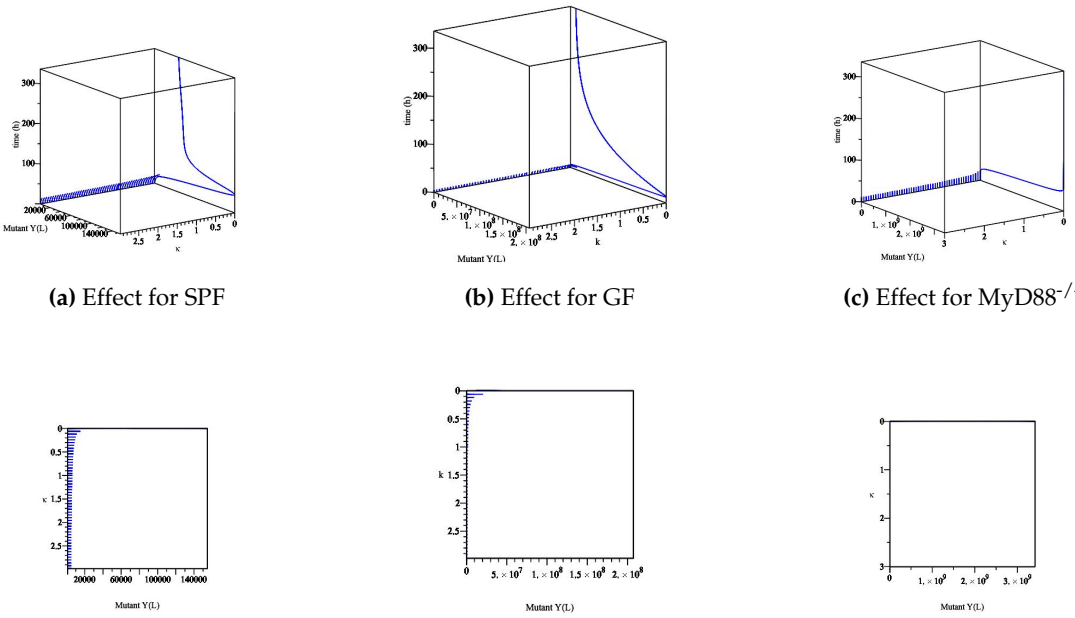

(a) Effect for SPF **(b)** Effect for GF **(c)** Effect for MyD88$^{-/-}$

(d) Projection for SPF **(e)** Projection for GF **(f)** Projection for MyD88$^{-/-}$

Figure 9. The sensitivity of the parameter κ in elimination of the mutant *Yersinia* strain in the lumen.

2. We calculate compartments $\mathcal{F}_i(x)$ defined as the rate of the appearance of new infections, $\mathcal{V}_i^+$ as the rate of transfer of individuals into compartment, and $\mathcal{V}_i^-$ as the rate of transfer of individuals out of the compartment [25]
3. The basic reproduction number is achieved as the spectral radius of the matrix $FV^{-1} = \rho\left(FV^{-1}\right)$ where $F = \frac{\partial \mathcal{F}_i(x_0)}{\partial x_j}$ and $V = \frac{\partial \mathcal{V}_i(x_0)}{\partial x_j}$.

Appendix B. Data Availability

1. The Matlab script
2. The Maple workbook
3. The described model is available in SBML format [31] (Level 3 Version 2 [32]) from BioModels database [33] under model identifier `MODEL2002070001`.

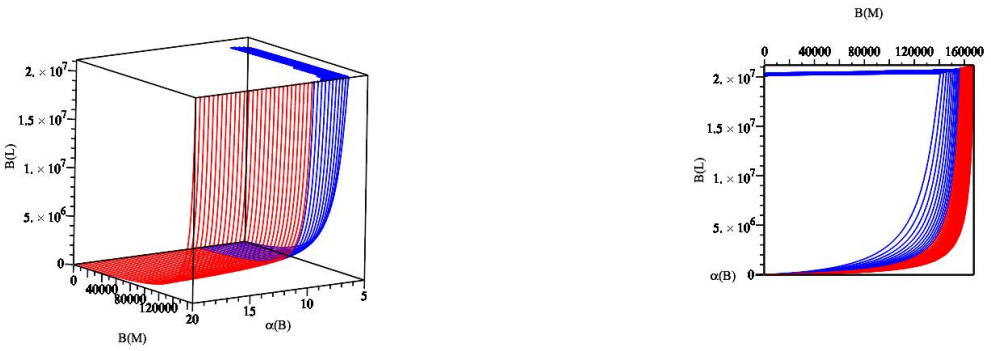

(a) The appearance of disease-free state **(b)** The projection of disease-free state

Figure 10. Diagram displaying the disease-free state by fixing the parameter values Ye SPF wt/A0 table 3 in model eq. (14). As long as the $\alpha^{(B)}$ is large enough, the disease-free state persists. However, by the reduction in $\alpha^{(B)}$, the basic reproduction number $\mathcal{R}_0^{wt}$ reaches its threshold value ($\mathcal{R}_0^{wt} = 1$). This causes changes in the dynamic behavior of the model eq. (14) as shown in fig. 3.

References

1. El Tahir, Y.; Skurnik, M. YadA, the multifaceted *Yersinia* adhesin. *International Journal of Medical Microbiology* **2001**, *291*, 209–218.
2. Handley, A.J.; Koster, R.; Monsieurs, K.; Perkins, G.D.; Davies, S.; Bossaert, L. European Resuscitation Council Guidelines for Resuscitation 2005: Section 2. Adult basic life support and use of automated external defibrillators. *Resuscitation* **2005**, *67*, S7–S23.
3. Mühlenkamp, M.; Oberhettinger, P.; Leo, J.C.; Linke, D.; Schütz, M.S. *Yersinia* adhesin A (YadA)–beauty & beast. *International Journal of Medical Microbiology* **2015**, *305*, 252–258.
4. Young, G.A.; LaVon, G.D.; Taylor, G.W. High efficiency absorbent articles for incontinence management. *Google Patents* **1992**. US Patent 5,147,345.
5. Pepe, G.J.; Albrecht, E.D. Actions of placental and fetal adrenal steroid hormones in primate pregnancy. *Endocrine reviews* **1995**, *16*, 608–648.
6. Cornelis, G.R. *Yersinia* type III secretion: send in the effectors. *The Journal of cell biology* **2002**, *158*, 401.
7. Ruckdeschel, K.; Roggenkamp, A.; Schubert, S.; Heesemann, J. Differential contribution of *Yersinia enterocolitica* virulence factors to evasion of microbicidal action of neutrophils. *Infection and immunity* **1996**, *64*, 724–733.
8. Lupp, C.; Robertson, M.L.; Wickham, M.E.; Sekirov, I.; Champion, O.L.; Gaynor, E.C.; Finlay, B.B. Host-mediated inflammation disrupts the intestinal microbiota and promotes the overgrowth of Enterobacteriaceae. *Cell host & microbe* **2007**, *2*, 119–129.
9. Stecher, B.; Robbiani, R.; Walker, A.W.; Westendorf, A.M.; Barthel, M.; Kremer, M.; Chaffron, S.; Macpherson, A.J.; Buer, J.; Parkhill, J.; others. Salmonella enterica serovar typhimurium exploits inflammation to compete with the intestinal microbiota. *PLoS Biol* **2007**, *5*, e244.
10. Geißert, J.; Bohn, E.; Mostolizadeh, R.; Dräger, A.; Autenrieth, I.; Beier, S.; Deusch, O.; Eichner, M.; Schütz, M. Model-based prediction of bacterial population dynamics in gastrointestinal infection. *bioRxiv* **2020**.
11. Nowak, M.; Robert, M. May. Superinfection and the evolution of parasite virulence. *Proc. R. Soc. B* **1994**, *255*, 81n89.
12. Castillo-Chavez, C.; Velasco-Hernández, J.X. On the relationship between evolution of virulence and host demography. *Journal of theoretical biology* **1998**, *192*, 437–444.
13. Dye, C.; Williams, B.G.; Espinal, M.A.; Raviglione, M.C. Erasing the world's slow stain: strategies to beat multidrug-resistant tuberculosis. *Science* **2002**, *295*, 2042–2046.
14. Boldin, B.; Geritz, S.A.; Kisdi, É. Superinfections and adaptive dynamics of pathogen virulence revisited: a critical function analysis. *Evolutionary Ecology Research* **2009**, *11*, 153–175.
15. Liu, W.m.; Hethcote, H.W.; Levin, S.A. Dynamical behavior of epidemiological models with nonlinear incidence rates. *Journal of mathematical biology* **1987**, *25*, 359–380.
16. Madden, L.V.; Hughes, G.; Van Den Bosch, F. *The study of plant disease epidemics*; Am Phytopath Society, 2007.
17. Gross, K.L.; Porco, T.C.; Grant, R.M. HIV-1 superinfection and viral diversity. *Aids* **2004**, *18*, 1513–1520.
18. Nurtay, A.; Hennessy, M.G.; Sardanyés, J.; Alsedà, L.; Elena, S.F. Theoretical conditions for the coexistence of viral strains with differences in phenotypic traits: a bifurcation analysis. *Royal Society open science* **2019**, *6*, 181179.
19. Mostolizadeh, Reihaneh, S.E.; Afsharnezhad, Z. Hopf Bifurcation and Chaos in a model for HTLV-I infection of CD4 + T- cells. *Annals of the Tiberiu Popoviciu Seminar of Functional Equations, Approximation and Convexity - Series B: Mathematical Interdisciplinary Research* **2017**, *15*, 59–79.
20. Mostolizadeh, R.; Afsharnezhad, Z. Hopf bifurcation in a model for adult T-cell leukemia. *Mathematical Methods in the Applied Sciences* **2018**, *41*, 6210–6225.
21. Shamsara, E.; Mostolizadeh, R.; Afsharnezhad, Z. Transcritical bifurcation of an immunosuppressive infection model. *Iranian Journal of Numerical Analysis and Optimization* **2016**, *6*, 1–16.
22. Hethcote, H.W. The mathematics of infectious diseases. *SIAM review* **2000**, *42*, 599–653.
23. Anderson, R.M.; May, R. Infectious diseases of humans. 1991. *New York: Oxford Science Publication Google Scholar* **1991**.

24. Diekmann, O.; Heesterbeek, J.A.P.; Metz, J.A. On the definition and the computation of the basic reproduction ratio R 0 in models for infectious diseases in heterogeneous populations. *Journal of mathematical biology* **1990**, *28*, 365–382.
25. van den Driessche, P.; Watmough, J. Reproduction numbers and sub-threshold endemic equilibria for compartmental models of disease transmission. *Mathematical biosciences* **2002**, *180*, 29–48. doi:10.1016/S0025-5564(02)00108-6.
26. Buonomo, B. A note on the direction of the transcritical bifurcation in epidemic models. *Nonlinear Anal Model Control* **2015**, *20*, 38–55.
27. Guckenheimer, J.; Holmes, P. *Nonlinear oscillations, dynamical systems, and bifurcations of vector fields*; Vol. 42, Springer Science & Business Media, 2013.
28. Wiggins, S. *Introduction to applied nonlinear dynamical system and chaos, Spring-Verlag, New York*; Inc, 1990.
29. Kuznetsov, Y.A. *Elements of applied bifurcation theory*; Vol. 112, Springer Science & Business Media, 2013.
30. Kuznetsov, Y.A. Practical computation of normal forms on center manifolds at degenerate Bogdanov–Takens bifurcations. *International Journal of Bifurcation and Chaos* **2005**, *15*, 3535–3546.
31. Keating, S.M.; Waltemath, D.; König, M.; Zhang, F.; Dräger, A.; Chaouiya, C.; Bergmann, F.T.; Finney, A.; Gillespie, C.S.; Helikar, T.; Hoops, S.; Malik-Sheriff, R.S.; Moodie, S.L.; Moraru, I.I.; Myers, C.J.; Naldi, A.; Olivier, B.G.; Sahle, S.; Schaff, J.C.; Smith, L.P.; Swat, M.J.; Thieffry, D.; Watanabe, L.; Wilkinson, D.J.; Blinov, M.L.; Begley, K.; Faeder, J.R.; Gómez, H.F.; Hamm, T.M.; Inagaki, Y.; Liebermeister, W.; Lister, A.L.; Lucio, D.; Mjolsness, E.; Proctor, C.J.; Raman, K.; Rodriguez, N.; Shaffer, C.A.; Shapiro, B.E.; Stelling, J.; Swainston, N.; Tanimura, N.; Wagner, J.; Meier-Schellersheim, M.; Sauro, H.M.; Palsson, B.; Bolouri, H.; Kitano, H.; Funahashi, A.; Hermjakob, H.; Doyle, J.C.; Hucka, M.; Adams, R.R.; Allen, N.A.; Angermann, B.R.; Antoniotti, M.; Bader, G.D.; Červený, J.; Courtot, M.; Cox, C.D.; Dalle Pezze, P.; Demir, E.; Denney, W.S.; Dharuri, H.; Dorier, J.; Drasdo, D.; Ebrahim, A.; Eichner, J.; Elf, J.; Endler, L.; Evelo, C.T.; Flamm, C.; Fleming, R.M.T.; Fröhlich, M.; Glont, M.; Gonçalves, E.; Golebiewski, M.; Grabski, H.; Gutteridge, A.; Hachmeister, D.; Harris, L.A.; Heavner, B.D.; Henkel, R.; Hlavacek, W.S.; Hu, B.; Hyduke, D.R.; Jong, H.; Juty, N.; Karp, P.D.; Karr, J.R.; Kell, D.B.; Keller, R.; Kiselev, I.; Klamt, S.; Klipp, E.; Knüpfer, C.; Kolpakov, F.; Krause, F.; Kutmon, M.; Laibe, C.; Lawless, C.; Li, L.; Loew, L.M.; Machne, R.; Matsuoka, Y.; Mendes, P.; Mi, H.; Mittag, F.; Monteiro, P.T.; Natarajan, K.N.; Nielsen, P.M.F.; Nguyen, T.; Palmisano, A.; Pettit, J.; Pfau, T.; Phair, R.D.; Radivoyevitch, T.; Rohwer, J.M.; Ruebenacker, O.A.; Saez-Rodriguez, J.; Scharm, M.; Schmidt, H.; Schreiber, F.; Schubert, M.; Schulte, R.; Sealfon, S.C.; Smallbone, K.; Soliman, S.; Stefan, M.I.; Sullivan, D.P.; Takahashi, K.; Teusink, B.; Tolnay, D.; Vazirabad, I.; Kamp, A.v.; Wittig, U.; Wrzodek, C.; Wrzodek, F.; Xenarios, I.; Zhukova, A.; Zucker, J. SBML Level 3: an extensible format for the exchange and reuse of biological models. *Molecular Systems Biology* **2020**, *16*, e9110, [https://www.embopress.org/doi/pdf/10.15252/msb.20199110]. doi:10.15252/msb.20199110.
32. Hucka, M.; Bergmann, F.T.; Chaouiya, C.; Dräger, A.; Hoops, S.; Keating, S.M.; König, M.; Le Novère, N.; Myers, C.J.; Olivier, B.G.; Sahle, S.; Schaff, J.C.; Sheriff, R.; Smith, L.P.; Waltemath, D.; Wilkinson, D.J.; Zhang, F. Systems Biology Markup Language (SBML) Level 3 Version 2 Core Release 2. *Journal of Integrative Bioinformatics* **2019**, *16*, 1. doi:10.1515/jib-2019-0021.
33. Malik-Sheriff, R.S.; Glont, M.; Nguyen, T.V.N.; Tiwari, K.; Roberts, M.G.; Xavier, A.; Vu, M.T.; Men, J.; Maire, M.; Kananathan, S.; Fairbanks, E.L.; Meyer, J.P.; Arankalle, C.; Varusai, T.M.; Knight-Schrijver, V.; Li, L.; Dueñas-Roca, C.; Dass, G.; Keating, S.M.; Park, Y.M.; Buso, N.; Rodriguez, N.; Hucka, M.; Hermjakob, H. BioModels—15 years of sharing computational models in life science. *Nucleic Acids Research* **2020**, *48*, D407–D415. doi:10.1093/nar/gkz1055.